Progress in Preparing Scenarios for ITER Operation

A.C.C. Sips[1,2], G. Giruzzi[3], S. Ide[4], C. Kessel[5], T.C. Luce[6], J.A. Snipes[7], J.K. Stober[8]

and the Integrated Operation Scenario Topical Group of the ITPA.

[1] JET-EFDA, Culham Science Centre, Abingdon OX14 3DB, UK.

[2] European Commission, Brussels, Belgium.

[3] CEA, IRFM, Cadarache F-13108 Saint- Paul-l Lez- Durance, France.

[4] Japan Atomic Energy Agency, 801-1 Muko-yama, Naka, Ibaraki 311-0193, Japan.

[5] Plasma Physics Laboratory, Princeton University, Princeton, USA.

[6] General Atomics, San Diego, USA.

[7] ITER Organization, 13115 Saint Paul Lez Durance, France.

[8] Max-Planck-Institut für Plasmaphysik, EURATOM-Association, D-85748, Garching, Germany.

e-mail contact of the main author: george.sips@jet.efda.org

(Figures will appear in colour in the online version only)

Abstract

The development of operating scenarios is one of the key issues in the research for ITER which aims to achieve a fusion gain (Q) of ~ 10, while producing 500 MW of fusion power for ≥ 300 s. The ITER Research Plan proposes a success oriented schedule starting in hydrogen and helium, to be followed by a nuclear operation phase with a rapid development towards Q ~ 10 in deuterium/tritium. The Integrated Operation Scenarios Topical Group of the ITPA initiates joint activities among worldwide institutions and experiments to prepare ITER operation. Plasma formation studies report robust plasma breakdown in devices with metal walls over a wide range of conditions, while other experiments use an inclined EC launch angle at plasma formation to mimic the conditions in ITER. Simulations of the plasma burn-through, predict that at least 4 MW of Electron Cyclotron heating (EC) assist would be required in ITER. For H-modes at q_{95} ~ 3 many experiments have demonstrated operation with scaled parameters for the ITER baseline scenario at n_e/n_{GW} ~ 0.85. Most experiments, however, obtain stable discharges at $H_{98(y,2)}$ ~ 1.0 only for β_N = 2.0 – 2.2. For the rampup in ITER early X-point formation is recommended, allowing auxiliary heating to reduce the flux consumption. A range of plasma inductance ($l_i(3)$) can be obtained from 0.65 to 1.0, with the lowest values obtained in H-mode operation. For the rampdown, the plasma should stay diverted maintaining H-mode together with a reduction of the elongation from 1.85 to 1.4. Simulations show that the proposed rampup and rampdown schemes developed since 2007 are compatible with the present ITER design for the poloidal field coils. At 13 – 15 MA and densities down to n_e/n_{GW} ~ 0.5, long pulse operation (> 1000 s) in ITER is possible at Q ~ 5, useful to provide neutron fluence for Test Blanket Module assessments. ITER scenario preparation in hydrogen and helium requires high input power (> 50 MW). H-mode operation in helium may be possible at input powers above 35 MW at a toroidal field of 2.65 T, for

studying H-modes and ELM mitigation. In hydrogen, H-mode operation is expected to be marginal, even at 2.65 T with 60 MW of input power. Simulation code benchmark studies using hybrid and steady state scenario parameters have proved to be a very challenging and lengthy task of testing suites of codes, consisting of tens of sophisticated modules. Nevertheless, the general basis of the modelling appears sound, with substantial consistency among codes developed by different groups. For a hybrid scenario at 12 MA the code simulations give a range for Q = 6.5 – 8.3, using 30MW NBI and 20MW ICRH. For non-inductive operation at 7 – 9 MA the simulation results show more variation. At high edge pedestal pressure (T_{ped} ~ 7 keV) the codes predict Q = 3.3 – 3.8 using 33 MW NB, 20 MW EC and 20 MW IC to demonstrate the feasibility of steady-state operation with the day-1 heating systems in ITER. Simulations using a lower edge pedestal temperature (~ 3 keV) but improved core confinement obtain Q = 5 – 6.5, when ECCD is concentrated at mid-radius and ~20 MW off-axis current drive (ECCD or LHCD) is added. Several issues remain to be studied, including plasmas with dominant electron heating, mitigation of transient heat loads integrated in scenario demonstrations and (burn) control simulations in ITER scenarios.

I. Introduction

The basic operational scenarios proposed [1] include the so-called baseline or reference scenario, which targets fusion gain Q ~ 10 using a conventional ELMy H-mode discharge at 15 MA plasma current and a toroidal field of 5.3 T (with a safety factor at 95 % flux, $q_{95} = 3$). Second, the hybrid scenario targets a high neutron fluence mission at reduced plasma current (~ 12 MA), operating with enhanced stability and plasma confinement with Q in the range 5 – 10. Third, the steady-state scenario, aiming at non-inductive operation at lower plasma currents (~ 9 MA) with enhanced confinement and stability, in order to obtain a target Q ~ 5. An 'advanced inductive' scenario may be used in ITER to investigate ignited or near-ignited plasmas at $Q \geq 20$ and 700 MW fusion power output, by combining operation at 15 MA with the increased plasma stability limits characteristic of so-called hybrid operation [2].

The ITER Research Plan (IRP) addresses the main mission goals: 1) to obtain plasma dominated by α-particle heating, 2) to produce a significant fusion gain ($Q \geq 10$), and 3) to achieve steady-state operation of a tokamak at $Q \geq 5$ for a pulse length up to 3000 s, while retaining the possibility of exploring 'controlled ignition' ($Q \geq 20$). Moreover, ITER operation will demonstrate integrated operation of technologies for a fusion power plant, test components required for a reactor and test concepts for tritium breeding modules. The research plan allows programme logic to be developed and key operational challenges to be identified and addressed during construction while exploring the issues in burning plasma physics likely to be encountered on route to Q ~ 10. The IRP proposes a sequence of plasma operation in hydrogen, helium, deuterium and ultimately deuterium-tritium mixtures for fusion power production.

During the last decade many experiments have been performed on devices with different first wall components. Metallic wall components, similar to those planned for ITER, have been tested, ranging from a few tungsten (W) tiles in the divertor (AUG in the late 1990's and JT-60U), to full coverage (AUG: W and C-Mod: Molybdenum). JET has tested an ITER-Like Wall configuration with Be walls and a W divertor. Other experiments have continued to use full graphite coverage; DIII-D in particular. The results from AUG, C-Mod, DIII-D, JET and JT-60U provide insight to the differences in operation and the results obtained in preparing ITER operating scenarios. Key parts of the ITER scenarios are determined by the capability of the proposed poloidal field (PF) coil set [3]. They include the plasma breakdown at low loop voltage, the current rise phase, the performance during the flat top phase and a ramp down of the plasma. The ITER discharge evolution has been verified in dedicated (joint) experiments. In recent experiments, the main focus of scenario studies has been the preparation of the baseline scenario and hybrid scenarios at high beta, demonstrating the feasibility of obtaining these regimes within the constraints of the device.

Predictions for ITER operating scenarios have been developed for many years. Some of the scenario modelling has been coordinated by the "Integrated Operating Scenario" topical group (IOS-TG) of the International Tokamak Physics Activity (ITPA). The goals of these integrated simulations are to establish a physics basis for the proposed operating modes in ITER, in conjunction with the results from recent tokamak experiments. Since it is not possible to reproduce all the physics parameters of ITER plasmas simultaneously in present experiments, simulations are used to project to ITER regimes using theory based physics models that are being tested against present tokamak experiments [4], [5] and [6]. These efforts include energy, particle, current, and momentum transport and self-consistent ideal magneto-hydrodynamic (MHD) equilibrium and stability calculations, together with heating

and current drive (H&CD) source models in time-dependent discharge simulations. In order to provide a more consistent prediction for ITER, a common set of parameters for the scenarios and a comparison (benchmarking) of the various codes has been coordinated by the IOS-TG. These activities involve the comparison of 1.5D core transport modelling assumptions and source physics modelling assumptions. The simulations focus on code to code results when using the same energy transport model, and within the same code when using different energy transport models. Recently, fully non-inductive scenario simulations include linear, ideal MHD stability analyses [7], aimed at defining an operational space for stable, steady-state operation in ITER. Developing and implementing particle transport models for scenario simulations has made good progress. Various approaches to particle transport modelling are used in predicting scenarios for ITER; from assuming the density profile to full core and scrape-off-layer particle transport models. The focus of future studies will be to include comprehensive models for the electron density evolution and (high-Z) impurity transport.

The ITER Research Plan is presented in section II, emphasising the issues that should be addressed prior to starting ITER operation. In section III, the latest results of dedicated experiments on plasma formation are given, as well as studies of the current rampup and rampdown phases and demonstration discharges that would scale to operation at Q ~ 10 in ITER. In section IV the progress in scenario modelling is presented with benchmarking studies for plasma scenarios in ITER. Non-active operation has been modelled providing information on the operational space available in hydrogen and helium. The ITER baseline scenario has been modelled, including the current rampup, the start of burn and rampdown phase. Finally, scenario explorations with the simulation codes are presented, providing insight to the achievability of steady state operation in ITER, depending on the (edge

pedestal) assumptions made. In section V the main limitations in experiments and scenario simulations are given, together with open issues and future research directions. Finally, the main conclusions are presented in section VI.

II. Preparing for ITER Operation

Now that the detailed ITER design is in its final stages and construction has begun, the ITER Research Plan (IRP) [8] is evolving to take into account cost and schedule constraints on the installation of in-vessel components, diagnostics and plant systems to effectively prepare operation and develop the physics program necessary to achieve the ITER project goals. To reduce costs, ITER is expected to have only one divertor protected by tungsten tiles up through at least the first DT experiments to reach Q = 10.

A. ITER research plan

The ITER Research plan envisages the following operation phases: First plasma, H/He operation, D operation, short pulse DT and long pulse DT operation, separated by shutdowns to complete hardware installation, maintenance and commissioning.

A.1 First plasma

First plasma has been defined as achieving a plasma current of at least 100 kA for at least 100 milliseconds. The purpose of this first operational milestone is to demonstrate that all systems required for plasma initiation are functional. The first plasma may be carried out at half toroidal field (TF) of 2.65 T or possibly at the full TF of 5.3 T. Only gas fuelling will be available in H or He. The disruption and runaway electron mitigation system will not be

available. Inboard or outboard plasma initiation may be attempted with circular or low elongation plasmas. Up to 6.7 MW of electron cyclotron (EC) heating power is expected to be available, using either fundamental or 2nd harmonic heating to assist the plasma formation at 5.3 T and 2.65 T respectively. Following first plasma, the poloidal field coils, central solenoid coils and toroidal field coils will be tested without plasma up to nominal performance.

A.2 H/He operation

The next operation phase will be with H and He plasmas and is expected to start at 2.65 T. The plasma current will be gradually raised up to 7.5 MA. Note that it will only be possible to limit the plasma on the high heat flux beryllium first wall panels in ohmic plasmas up to a plasma current of about 4.5 MA before exceeding their steady-state heat flux capability of 4.7 MW/m^2. This non-active operation phase is required to bring the tokamak plasma and plant systems up to nominal performance, to investigate disruption loads and to commission the disruption mitigation system (DMS) as the plasma current is progressively raised to 15 MA prior to machine activation. Attempts will be made to achieve H-mode in He plasmas with up to 60 MW of auxiliary heating power using neutral beam injection (NBI), EC, and ion cyclotron (IC) heating. This is based on the observation of a lower threshold in helium plasmas compared to hydrogen found in AUG [9], DIII-D [10] and JET [11]. Note that it is planned to install the first ferromagnetic test blanket modules (TBMs) prior to this operation phase.

A.3 D operation

Once the tritium plant is sufficiently commissioned and nuclear regulatory approval has been obtained, plasma operation in deuterium will be possible. The purely D operation phase is

expected to be relatively short with the gradual introduction of small amounts of T to quickly gain experience with DT plasmas and increase performance as auxiliary heating systems and plasma control development allows.

A.4 DT operation

The amount of tritium will be gradually increased as heating systems improve performance and first wall and divertor heat load protection systems are developed to allow increased plasma performance, culminating in short pulse (10's of seconds) 50/50 DT mixture operation at high performance (up to Q ~ 10). The following DT campaigns will attempt to reach the project goal of demonstrating ≥ 300 s of fusion burn duration at Q = 10. Also long pulse hybrid operation and possibly long pulse non-inductive operation will be attempted within the limits of the installed heating and current drive systems.

B. High priority research issues for ITER scenarios

On-going research and development of ITER scenarios on existing experiments and through joint modelling activities is an important part of preparation for ITER operation. Understanding of the physics issues that ITER must face, gained now, will improve the efficiency of ITER operation. While some issues can only be addressed on ITER itself, a number of operational scenario issues can be addressed on existing devices and be compared with modelling results.

With the choice of a single all-tungsten divertor up through high performance plasmas, additional experiments need to be performed to assess how fast the plasma current can be ramped up and how soon the plasma can be diverted with a high-Z divertor. Understanding

the density range that can be covered for a given plasma current ramp rate and the resulting evolution of Z_{eff} are also important to develop current rise scenarios for ITER. For the early-diverted plasma scenarios required for ITER, it is also important to understand the limits of internal inductance versus edge q value in comparison with the well-known operational space limits for limited plasmas in the current rise [12]. It is also important to develop high-Z divertor heat flux control schemes on existing devices at high performance.

Key in scenario predictions for ITER is the validation of transport models used and verification of the assumptions made for the boundary (pedestal) conditions in the calculations. In addition, validation is required of the various codes that have implemented the transport and pedestal models. This is important for all phases of the ITER discharge, including the current rise phase, flat top phase and rampdown phase as the transport and pedestal model assumptions critically affect the predictions for fusion performance, current density profile evolution, achievable pulse length and the requirements (capabilities) for the heating and current drive systems together with the control of the plasmas in ITER. Details of the assumptions made for the pedestal have been given in this paper.

Through modelling benchmarked with existing experiments, it is possible to validate and project the current drive capability of each of the proposed auxiliary heating systems for ITER. While it is not possible to demonstrate the current drive efficiency at ITER parameters in existing devices, validation of current drive models has been carried out and extrapolation to ITER conditions can be done with high confidence. It is important to understand how the three baseline H&CD systems can shape or maintain the current density for a range of expected temperature and density profiles in order to assess the need for upgrades, such as lower hybrid heating and current drive for long pulse operation.

While much R&D has been done, continued refinement of ITER inductive, hybrid, and steady-state DT scenarios is necessary to properly model a range of possible operational scenarios for ITER. It is important to include realistic H&CD source models for a range of particle and energy transport assumptions. These results in comparison with initial experiments on ITER will help to guide the experimental program to make efficient use of the limited run time that will be available on ITER.

Previous emphasis has been on the high performance DT scenarios, but it is also important to model early operational H/He and D scenarios at both full and half TF and compare with the results of existing experiments. It is important to understand what early L-mode results ITER can expect for a wide range of transport models to be able to quickly assess ITER results against expectations and guide the operational program. Even at low performance, an assessment of the expected H&CD efficiency for a range of conditions will allow early comparison with ITER results to plan for future upgrades to H&CD systems. Comparison of early ITER results with a range of transport models will also allow an early assessment of expectations for later high performance operation to better guide the experimental program.

Development on existing devices of kinetic profile control schemes with simultaneous control of multiple plasma parameters with shared actuators including MHD mode control would also help reduce development time on ITER. Simultaneous control of the temperature profile with both internal and edge transport barriers as well as the current density profile over multiple current relaxation times may be required for high performance long pulse scenarios. One of the particular challenges for ITER is to develop simultaneous integrated scenario control of MHD modes, kinetic profiles, divertor and first wall heat flux, and

impurity and radiation control with a limited set of shared actuators. Any development of even parts of such simultaneous control would help reduce the limited available development time on ITER. This requires the development of sophisticated plasma control models as well as demonstration of at least parts of such simultaneous control on existing experiments.

III. Demonstrating ITER scenarios

A. Plasma formation

On ITER, the superconducting central solenoid (CS) and the thick vessel walls limit the toroidal electrical field available for plasma breakdown to ~ 0.30 – 0.35 V/m, which is well below the values used in most of the operating tokamaks. Since ITER is significantly larger than these tokamaks one might argue that the connection length is longer and breakdown should be possible at a lower electrical field. Such an argument neglects the quality of the field null which is not easy to predict, especially in the presence of eddy currents in ferromagnetic in-vessel shielding, TBMs, and other components. Experiments on JET [13], DIII-D [14], KSTAR [15] and Tore Supra (TS) [16] show that ohmic plasma startup with the electric field value of ITER (0.3 V/m) is marginally possible for optimized magnetic configurations. Data from existing machines at least do not show a clear size scaling of the electric field necessary for ohmic breakdown.

The ionisation of the filling gas and the burn-through is dominated by the conditions of the main chamber first wall, which will be made of beryllium in ITER. Some devices with carbon fibre composite (CFC) walls require conditioning following disruptions or following

operation close to the density limit. However, no experiments report significant problems with plasma initiation for Be or high-Z walls. After a tokamak with metal walls is conditioned for operations, reliable plasma initiation can be maintained without inter-pulse glow discharge cleaning (GDC), even after disruptions. However, with the Be-wall at JET sufficient gas fuelling was required during the plasma formation phase to avoid runaway electron build-up [17].

Assisting plasma startup by electron cyclotron heating (ECH) is highly desirable for ITER to increase the operational margin [18]. The relevance of ECH assistance is highlighted by the first experiments on KSTAR in 2008: ECH assistance was necessary to breakdown the first plasmas [19]. This access route to plasma formation was successively optimized and in 2010 even purely ohmic startup was achieved. A similar development route may be required in ITER. ECH-assisted breakdown can either create a low-temperature plasma prior to the application of a loop voltage, or in the presence of a loop voltage, it may relax the Paschen criterion by additional acceleration of an otherwise sub-critical electron distribution [20]. In the subsequent current formation phase, when closed flux surfaces form and the electron temperature rises, ECR heating of the electrons can facilitate the sustainment of the breakdown through the radiation barrier when light impurities are ionized and radiate a significant fraction of the ohmic heating power. In this case the ECH provides input power and results in a more rapid increase in electron temperature to overcome the radiation barrier due to low-Z impurities. An example of the effectiveness of ECH-assisted startup for burn-through of the radiation barrier at AUG is given in Figure 1, showing detailed measurements of impurities, plasma density and plasma current formation.

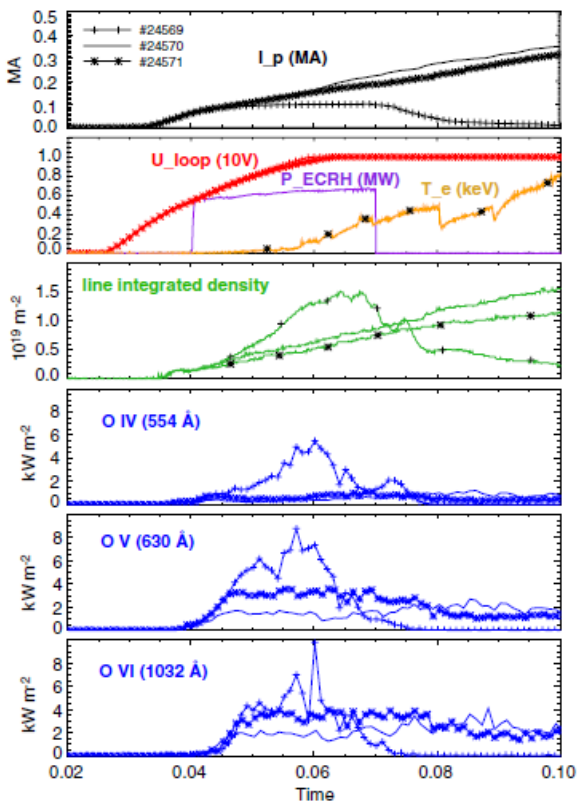

FIG. 1. *Sequence of successive plasma startups on AUG (~ 1 V/m). #24569 failed to sustain breakdown (time traces with crosses), in #24570 ECH was applied (time traces without symbols) and in #24571 breakdown was achieved without ECH due to conditioning effects of the previous discharge (time traces with stars). Line-averaged density is measured perpendicular in the midplane, as is the radiation from partially ionized oxygen, for which a SPRED VUV spectrometer is used. Other parameters such as field null and prefill were kept constant. Reproduced with permission from [J. Stober et al,"ECH-assisted plasma startup with toroidally inclined launch: multi-machine comparison and perspectives for ITER", Nucl. Fusion* ***51*** *(2011) 083031].*

In contrast to most of the present-day experiments that use ECH assisted startup, ITER will build up loop voltage prior to the formation of the field null due to the strong shielding by the vessel and will use an inclination of the EC beam of 20^{o}. Dedicated experiments have been performed in present devices studying the effect of toroidal inclination of the EC beam, with the participation of the tokamaks AUG (using X2), DIII-D (X2), FTU (using O1), KSTAR (X2), Tore Supra (O1, X2), HL-2A (O1) and of the stellarator TJ-II (X2). All devices that participated in these dedicated experiments could demonstrate ECH-assisted startup in the ITER-like mode, although in some cases the necessary power was almost a factor of 2 higher compared with perpendicular launch [18].

The DYON code is a plasma burn-through simulator developed at JET [21]. The simulation results have been compared and validated with experimental data from the JET campaigns with the ITER-like wall. The DYON code has been used to perform a predictive simulation for ITER [22]. Without EC-assist for plasma burn-through, the code predicts that startup in ITER will be possible only at very low prefill gas pressure (at $p(0) < 10^{-5}$ Torr). In JET with the ITER-like wall, such low prefill gas pressures are not used in order to avoid having a weak (and slow) electron avalanche phase or low initial plasma density that may lead to runaway electrons. However, 4 MW of RF assist is predicted to allow ITER startup available at prefill gas pressures up to 5×10^{-5} Torr, which is more typical in present devices. The EC assist should result in prompt deuterium burn-through. The simulation results indicate that the required ECH power for reliable startup increases almost linearly with prefill gas pressure. Reasonable levels (< 5 %) of Be content should not impact on plasma burn-through in ITER, but modest (~ 1 % to 2 %) C content can increase the radiated power significantly. The simulations indicate that ITER should keep the carbon concentration at plasma initiation below 0.5 % to have the full benefit from the Be-wall (consistent with results from the ITER-Like Wall in JET). Residual oxygen may form BeO layers on the first wall components in ITER. BeO has higher surface binding energy than the pure beryllium wall [23], making physical sputtering more difficult compared to pure beryllium. Sputtering of these layers has been observed in JET and leads to an oxygen content of < 0.5 % of the initial plasma, giving a radiation peak at a level similar to the deuterium ionisation peak [22].

B. ITER current rampup and rampdown phases

The current rampup and rampdown are critical phases of any ITER discharge, as the former establishes the plasma current and geometry prior to the burning phase, and the latter brings

the plasma out of the burning phase while reducing the plasma current and cross-section to avoid a disruptive termination. The emphasis here will be on the 15 MA baseline scenario. The current rampup for the baseline is anticipated to take from ~ 50 to 100 s with an X-point formation at ~ 4 MA after ~ 15s. The rampdown phase is predicted to take ~ 200 s using diverted plasmas.

Experimental activities on JET, DIII-D, C-Mod and ASDEX-U (AUG) were pursued from 2008 – 2012 to examine the rampup, flattop and rampdown phases of the ITER discharge [13]. These are done by creating a self-similar version of the ITER discharge at the reduced parameters of the present tokamaks (plasma current, toroidal field, plasma temperature and density, current diffusion time, energy confinement time, etc.) while matching dimensionless parameters such as q_{95}, β_N, n_e/n_{GW}, t_{ramp}/τ_{CR} and plasma shape to the extent possible (here $\beta_N = \beta /(I/aB)$ is the normalized beta, with a being the minor radius of the device, n_e the electron plasma density, n_{GW} the Greenwald density limit which scales as $I/\pi a^2$, t_{ramp} being the required to obtain the flat top value of the plasma current (I) and τ_{CR} the current diffusion time which is proportional to the effective ion charge and electron temperature (T_e) ; $\tau_{CR} \sim Z_{eff}\, T_e^{1.5}$). Discharges using early x-point formation were established to match ITER with a divert time of 15 s out of a 100 s rampup, and large bore plasma cross-sections were created as early as possible. For the rampup phase, the rise time was scaled by the current diffusion time, τ_{CR} being about 10 – 15 s for ITER during the rampup phase (note that τ_{CR} would be several hundred seconds during the flat top burn phase in ITER). Ohmic and heated rampups were examined, primarily in L-mode, although transitions to H-mode were observed. The experiments are intended to address the flux required, the current profile evolution, energy confinement, and impurity and radiation levels both with and without heating, and the impact of the ramp rate of the plasma current.

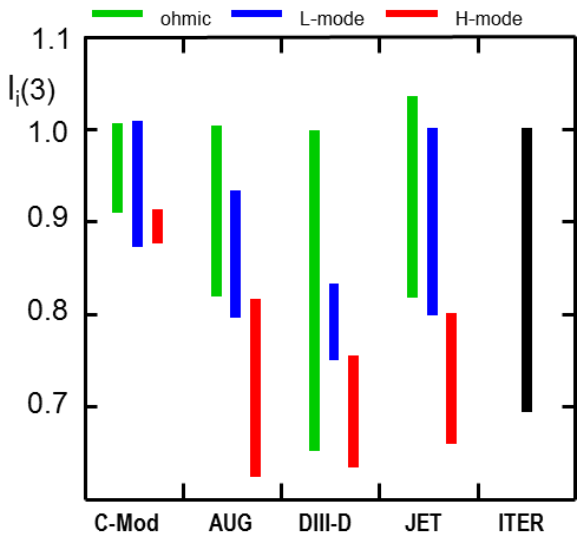

FIG. 2. *Variations in the plasma internal self-inductance, $l_i(3)$, in C-Mod, AUG, DIII-D, and JET for plasma current rampup ITER-like discharges, for ohmic, heated L-mode, and L-mode with an H-mode transition. Heating in L-mode can provide some reduction in l_i, although an H-mode transition provides a very strong reduction. The lowest values of l_i obtained in DIII-D induced MHD instability. Reproduced with permission from [A.C.C. Sips et al, "Experimental studies of ITER demonstration discharges", Nucl. Fusion* ***49*** *(2009) 085015].*

Experiments in JET and DIII-D [13] directly tested the impact of diverting progressively earlier. Having larger plasma cross-section after the breakdown and early x-point formation achieved lower l_i, which is more vertically stable to vertical motion. C-Mod produced large-bore plasmas and x-point formation at about 15 % of the total rampup time, similar to the ITER value, but did not vary this time. For ohmic discharges, the plasma current ramp rates were varied in JET, C-Mod, AUG, and DIII-D, made to correlate with 60 – 100 s rampup times in ITER, showing variations in $l_i(3)$ of 0.80 – 1.0 (faster-slower), while C-Mod showed a narrower range of 0.9 – 1.0. DIII-D could reach much lower values of l_i to 0.65, but these became MHD unstable. These ranges of $l_i(3)$ for the various tokamaks are shown in Figure 2, with ohmic, heated L-mode, and rampups with an H-mode. All devices observed increased

impurity content, higher Z_{eff}, when heating with the plasma on the limiters, regardless of location, justifying the earliest diverting of the plasma. The various tokamaks have different heating sources and power levels in their rampup experiments: AUG has used on and off-axis NB at 1.5 – 5 MW or ECH at 0.5 MW. JET has used ICRF at 2 – 6 MW, LH up to 2.2 MW, and NB up to 10 MW. C-Mod has used ICRF with 1 – 3 MW. DIII-D has used 1 – 5 MW of NB and up to 1.25 MW of ECH. With additional heating in the rampup, l_i is observed to be lower or similar to ohmic by the end of the rampup phase. In C-Mod the application of 1 – 3 MW of ICRF did not change the l_i value from ohmic, while JET observed l_i values that were slightly lower than ohmic, with the application of 3 MW of ICRF, 2.2 MW of LH, or 4 MW of NB. If the heating leads to an H-mode transition during the rampup even lower l_i values are reached, as well as some further reduction in the resistive consumption.

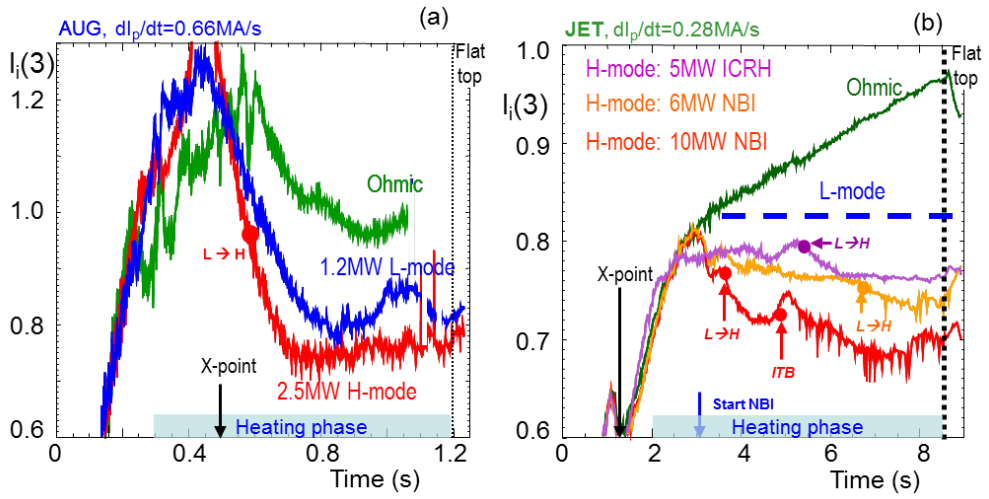

FIG. 3. *Time evolution of the plasma internal self-inductance, l_i, for AUG and JET, demonstrating the impact of an H-mode during the rampup phase, strongly broadening the current profile. The dashed blue line for JET represents the typical $l_i(3)$ value obtained with heating in L-mode without an H-mode transition. Reproduced with permission from [A.C.C. Sips et al, "Experimental studies of ITER demonstration discharges", Nucl. Fusion* ***49*** *(2009) 085015].*

Figure 3 shows time evolutions of l_i for the AUG and JET with the onset of H-mode resulting in a significant broadening of the current profile. Similar results have been obtained in DIII-D and C-Mod. Both DIII-D [24] and JET [13] demonstrated the ability to feedback control the value of l_i for inductive rampup, by varying the ramp rate or heating. Overall, experiments have indicated that the ITER baseline discharge should have the capability to keep the l_i value within a range that is vertically stable, by utilizing a large bore plasma following breakdown, by diverting as early as allowed by the PF coils, using the plasma current ramp rate and relatively low levels of heating in L-mode.

Volt-second savings with heating in L-mode are obtained in all devices due to a reduction in the resistive flux consumption, and possibly some reduction from the decrease in l_i (inductive). Shown in Figure 4 are the volt-second savings from DIII-D using NB and EC heating in L-mode [25], and C-Mod using ICRF in L-Mode and with an H-mode transition [26]. Greater reductions in the required flux usage can be obtained after an L to H-mode transition during the rampup, mainly due to from a reduction of l_i associated with the increased pedestal bootstrap current. These levels of volt-second reductions in the rampup phase are sufficient in magnitude to provide ITER with flattop durations of $\geq$ 300 s. For example, C-Mod [26] experiments indicated a 9.6 % level of savings over ohmic rampup with 1-2 MW of ICRF heating in L-mode, and 14.4 – 23 % level of savings if an H-mode occurred in the last 20 % of the rampup. These are determined by comparing the change in the poloidal magnetic flux at the plasma boundary for ohmic and heated rampups. Utilizing simulations of the ITER baseline current rampup [3], which required 115 Wb for an ohmic rampup (excludes external inductive), these translate into 11 and 17 – 23 Wb, respectively. DIII-D reports [24] and [27] indicate a savings level of ~ 20 % over ohmic rampups.

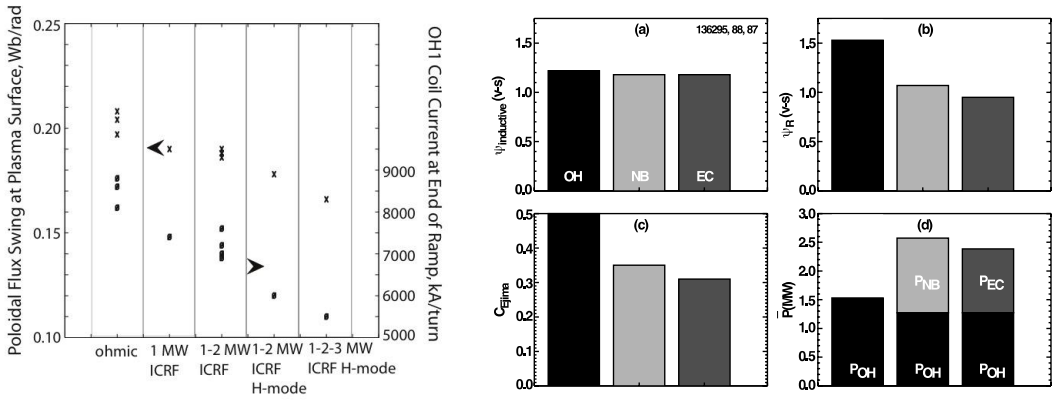

FIG. 4. *Reduction of the required volt-seconds for current rampup when applying heating compared to ohmic rampup, with ICRF heating of 1 – 2 MW in C-Mod, and with 1.35 MW of NB and 1.15 MW of EC heating in DIII-D. C-Mod showed no significant modification of l_i, and DIII-D shows only a minor change, indicating all the savings is due to a reduction of the resistive consumption. The left-figure is reproduced with permission from [C.E. Kessel et al, "Alcator C-Mod experiments in support of the ITER baseline 15 MA scenario", Nucl Fusion **53** (2013) 093021], The right-figure is reproduced with permission from [G. L. Jackson et al, "Understanding and predicting the dynamics of tokamak discharges during startup and rampdown", Phys. Plasmas **17** (2010) 056116].*

The rampdown phase in ITER has to reliably terminate the discharge, either from a scheduled end to a burning plasma or when it is necessary to stop the discharge following a request from the control systems. To allow maximum burn duration, no addition flux should be used during the rampdown phase. The reduction of the plasma current should be controlled and slow enough to avoid the plasma inductance from increasing to levels where it is not possible to maintain control over the vertical position of the plasma. Typically, the fusion power will reduce during the current rampdown, leading to a (sudden) H to L back transition, which leads to difficulties with controlling the radial position of the plasma. Ramp-down schemes should be developed and tested to cope with confinement transitions and to stay within the limits of the vertical stabilisation systems in ITER.

JET, DIII-D and C-Mod produced a range of rampdown experiments, and each reduced elongation from 1.7 – 1.8 down to ~ 1.4 – 1.5 as part of this rampdown in order to avoid vertical instability. JET [13] and DIII-D [28] created the same reduction in plasma cross-section anticipated on ITER, a reduction of the plasma height while maintaining the lower single null (SN) divertor configuration. C-Mod reduced the elongation while holding the diverted plasma on the midplane to allow ICRF heating throughout the rampdown. JET, DIII-D and C-Mod examined a range of ramp down rates for the plasma current, indicating that the slowest ramps could result in the CS current increasing rather than decreasing, while they provide the slowest increases in l_i.

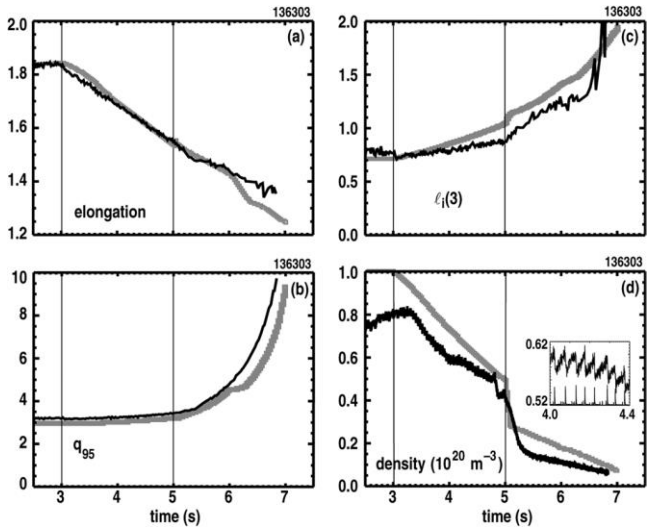

FIG. 5. *Current rampdown experiment in DIII-D established to imitate the simulation from DINA of the ITER rampdown phase. An H-mode is sustained from flattop into rampdown until 5 s, where auxiliary heating is terminated and an H-L transition occurs. Simultaneous with the current rampdown, the plasma elongation is reduced by moving the top of the LSN plasma downward and holding the divertor flux geometry as constant as possible. Reproduced with permission from [P.A. Politzer et al, "Experimental simulation of ITER rampdown in DIII-D", Nucl Fusion* ***50*** *(2010) 035011].*

DIII-D [28] constructed rampdowns to hold a fixed q_{95} and weakly rising l_i, during the heated H-mode phase for about half of the rampdown time. The results for DIII-D are shown in Figure 5. The NB heating power was then turned off and the plasma transitioned to L-mode, accompanied by a more rapid rise in q_{95} and l_i and strong reduction in density. C-Mod examined three rampdown rates (as shown in Figure 6), equivalent to 120 – 240 s in ITER, with ICRF heating that maintained EDA H-modes into the rampdown.

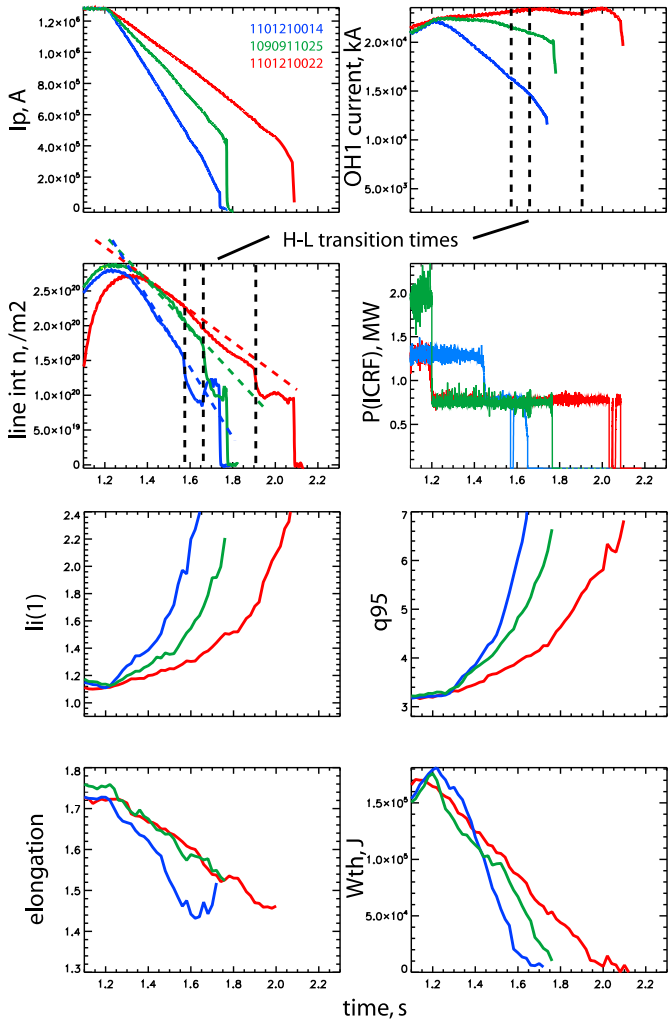

FIG. 6. *C-Mod rampdown discharges showing 3 cases with ITER-equivalent rampdown times of 120, 180, and 240 s. The vertical dashed lines indicate the time of the H to L transition, and the coloured dashed lines indicate the plasma current trajectory on top of the density trajectory. The slowest (red) case shows that the OH1 coil current does not decrease, and there is an over-current visible at the H to L transition. Reproduced with permission from*

*[C.E. Kessel et al, "Alcator C-Mod experiments in support of the ITER baseline 15 MA scenario", Nucl Fusion **53** (2013) 093021].*

The H-modes persisted to about 35 – 45 % of the flattop plasma current before a back transitioning to L-mode, in spite of continued ICRF injection. The slowest ramp rate resulted in continued flux consumption and ohmic coil current advance. The plasma density was found to decrease, while in an EDA H-mode, with the plasma current, keeping n_e/n_{GW} fixed, regardless of the ramp rate. It was found that faster ramps were preferred in order to guarantee that the CS coil over-current was insignificant when the H to L transition did eventually occur. No vertical stability issues on C-Mod were observed regardless of the rise in q_{95} or l_i during this phase. JET [29] performed several ohmic rampdowns to understand the relationship between the evolution of l_i, q_{95}, and elongation. This demonstrated that combinations of elongation reduction and current rampdown rate could be used to provide a stable rampdown phase. Heated rampdowns were also investigated and showed the H-mode phase could keep $l_i(3)$ between 1.0 and 1.2 for medium to slower ramp rates.

In general, a number of critical features of the current rampdown phase have been established. The H-mode can be robustly maintained into the rampdown at least to 2/3 – 1/2 of the flattop plasma current, thereby avoiding a CS over-current near the maximum CS current at end of flattop. The H-mode will ultimately transition back to L-mode, which can be induced by turning off auxiliary power or by falling below the L-H threshold (or some fraction if there is hysteresis). The plasma density falls with the plasma current in a H-mode with regular ELM behaviour.

Elongation reduction is clearly a necessary element of any current rampdown in order to maintain vertical stability directly and by helping the plasma stay in H mode by reducing the

surface area. At the high operating density for ITER, n_e/n_{GW} = 0.85, and with intentional impurities for core plasma radiation, it is still unclear how much power is required to sustain the H-mode in rampdown. Flattop experiments in C-Mod reached the n_e/n_{GW} range of 0.7 – 0.89, and could routinely maintain H-modes into the rampdown with ICRF heating; however, only small amounts of neon were used in some cases, so that further investigation is required.

C. Operating Experience in Present-Day Experiments at Conditions Required for Q ~ 10 in ITER

Metrics for dimensionless parameters to compare present-day experiments with conditions required to achieve the objectives of ITER have been established previously [30] and will be applied here. Generating 500 MW of fusion power at the full magnetic field of ITER (vacuum B = 5.3 T at R = 6.2 m) implies a volume-averaged pressure of ~ 3 x 10^5 Pascal must be stably confined. The normalized pressure β_N is used where ratio of the kinetic to magnetic pressure is normalized to a factor I/aB, which is found to characterize the scaling of the free-boundary stability limit of tokamaks (see [31] for heuristic arguments explaining this scaling and why it is not properly dimensionless). For a fixed size and B, this metric implies β_N/q_{95} needs to be 0.6 to achieve the necessary pressure in ITER or the equivalent metric in present-day machines. Stationary operation at Q = 10 implies that the auxiliary power cannot exceed 50 MW. Energy confinement time scalings have been developed from multi-tokamak databases. The two most commonly used are the ITER-89P scaling for global energy confinement time [32] and the IPB98y,2 scaling for thermal energy confinement time [33]. The ratio of the experimental confinement time to these scalings is denoted as H_{89P} and $H_{98(y,2)}$, respectively. Reaching Q = 10 at P_{fus} = 500 MW means $H_{98(y,2)}/q_{95}$ = 0.33 or H_{89P}/q_{95} = 0.7. Combining these to give a composite gain metric $G = \beta_N H /(q_{95})^2$, G must be 0.2 using

the IPB98y,2 scaling or 0.42 for the ITER-89P scaling. These metrics establish what operating conditions are required in present-day experiments to demonstrate plasma conditions relative to conventional energy confinement and known pressure and current limits in tokamaks.

The baseline scenario proposed for achieving these conditions in ITER is an H-mode plasma ($H_{98(y,2)} = 1$) at 15 MA ($q_{95} = 3$) with $\beta_N = 1.8$. Even though it may be possible to achieve the primary physics objective under different conditions, this is an appropriate choice for a baseline scenario, because it sets the engineering requirements for the facility. In the following, the recent experience in present-day experiments (Alcator C-Mod, AUG, DIII-D, and JET) with this baseline scenario will be discussed. Areas where the tokamaks provide complementary information and where the experience base is significantly different from ITER will be pointed out. The section will conclude with a discussion of possible alternative approaches to achieving the primary physics objective.

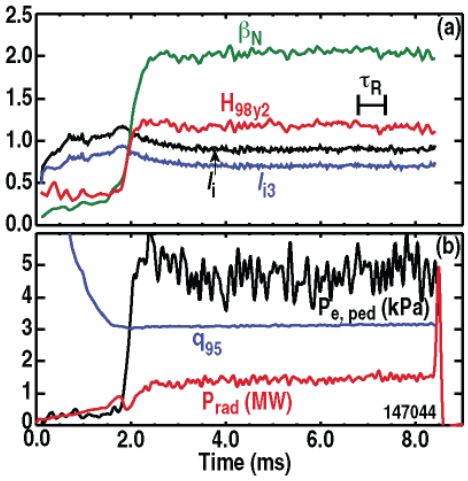

FIG. 7. *Demonstration of baseline scenario to resistive equilibrium in DIII-D. Reproduced with permission from [G.L. Jackson et al, "Long-pulse Stability Limits of ITER Baseline Scenario Plasmas in DIII-D", Proc. 24th Int. Conf. on Fusion Energy, San Diego, USA, 2012 (Vienna, IAEA) (2012) EX/P2-08].*

Conditions suitable for Q = 10 in ITER have been achieved in present-day experiments. Figure 7 shows an example from the DIII-D tokamak where stable conditions exceeding the

ITER requirements were obtained for many resistive relaxation times limited only by power supply limits, indicating truly stationary conditions [34]. Similar plasmas are obtained in JET [35], AUG [36] and Alcator C-Mod [26] across a broad range in plasma density.

The goal of the experiments in DIII-D was to simulate ITER conditions as closely as possible, scaling ITER parameters to the DIII-D tokamak; hence plasmas discharges of the type shown in Figure 7 form the physics basis of the ITER design point. The heating is due to co-injected neutral beams (co-NBI) that are also a source of central fuelling and torque that are much larger in relative terms than possible in ITER. The most stable operating region found to be $\beta_N \sim 2$. The wall material is graphite, which has a significant influence on the edge boundary conditions and divertor operation.

In recent years, facilities have undertaken hardware changes in order to explore plasma conditions in directions where ITER plasmas vary significantly from the established physics basis.

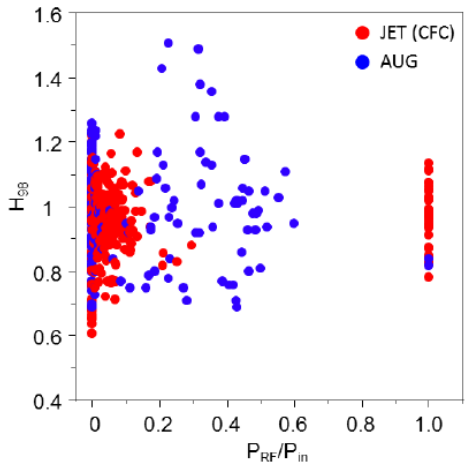

FIG. 8. *Effect of varying fraction of RF heating on confinement in AUG and JET is small. Reproduced with permission from [A.C.C. Sips et al, "Demonstrating the ITER Baseline Operation at q_{95} = 3", Proc. 24th Int. Conf. on Fusion Energy, San Diego, USA, 2012 (Vienna, IAEA) (2012) ITR/P1-11].*

Because the moment of inertia increases with size much more rapidly than the applied torque or momentum confinement time, it is expected that the ITER plasmas will rotate much more slowly than those in present-day experiments. The effect of this is explored in present-day experiments by using heating methods that do not apply torque. JET has used ion cyclotron resonant frequency heating (ICRF), while AUG has used ICRF and electron cyclotron heating (ECH). The limited data in the baseline scenario (see Figure 8) with a minority of the heating from these sources sees little change in the H factor.

C-Mod is unique in that the sole auxiliary heating is ICRF. The H factors in the baseline scenario are typically < 1. However, these plasmas are limited in the β_N achieved to a range 1.1 – 1.75 by the power available, so it is difficult to separate the effect of rotation due to external torque from the trends that the H is low at low P_{loss}/P_{LH} and at low β_N. DIII-D has applied both ECH and balanced NBI and sees a reduction in the H factor, although at ITER-relevant torque, it is still ~ 1. Reduction in applied torque also leads to a narrowing of the stable operating range in DIII-D. The limit to the operating range in DIII-D with reduced torque input is set by the onset of an $n = 1$ tearing mode during the phase just after the transition from ohmic to H mode for a range of $\beta_N = 1.5 – 2$ [37]. Pulses stable to m/n = 2/1 tearing modes have been demonstrated for a plasma inductance at the start of the heating ($l_{i,start}$) in the range $0.9 \leq l_{i,start} \leq 1.25$. For operation at ITER relevant torque (taken as ≤ 1 Nm) the stable range of operation is somewhat reduced as shown in Figure 9.

As mentioned above, wall materials play a significant role in setting the edge boundary conditions. DIII-D has retained a graphite wall and therefore serves a tie to the prior physics basis. C-Mod has always operated with a molybdenum first wall and has introduced recently tungsten (W) material in the divertor strike area. Spectroscopy indicated very little tungsten

entering the core plasma. This is consistent with the experience of AUG, which started with W divertor tiles and saw little contamination of the core. Taken together, it appears the main chamber material in AUG and C-Mod is the dominant source of high-Z impurity, not the divertor tiles.

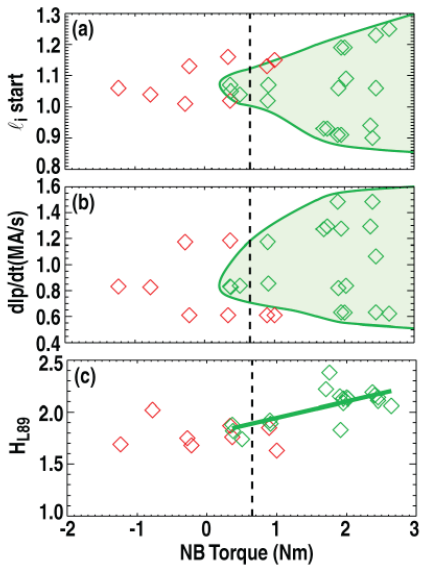

FIG. 9. *At lower applied torque, the operating space for the baseline scenario in DIII-D shrinks. The green shaded area shows the regions where stable operation is obtained from the specified initial conditions. Reproduced with permission from [G.L. Jackson et al, "Long-pulse Stability Limits of ITER Baseline Scenario Plasmas in DIII-D", Proc. 24th Int. Conf. on Fusion Energy, San Diego, USA, 2012 (Vienna, IAEA) (2012) EX/P2-08].*

Demonstration of the ITER reference scenario on AUG with its tungsten wall has been performed using central wave-heating (ECH or ICRF) to avoid core tungsten impurity accumulation [36]. Stable behaviour for many confinement times has been obtained at n_e/n_{GW} = 0.80 – 0.85 and energy confinement ($0.95 \leq H_{98(y,2)} < 1.05$) as long as β_N stayed above 2 (typically $2.0 < \beta_N < 2.2$) With less heating power, leading to a further reduction of β, the plasmas became more unstable. In such a situation the ELM frequency decreased, and a peaking of the central density set in. As long as the gas puff is sufficiently high, impurity accumulation could be avoided, but H-factors were below 0.9. Compared with results with a C-dominated wall the operation with the full-W wall in AUG is restricted to higher densities $f_{GW} > 0.75$ and confinement is on average reduced by 5 – 10 % [38]. Thus, the lowest H-factors obtained in AUG can be attributed to high gas puff levels required to avoid W-

accumulation. For the extrapolation to ITER however, the results of AUG-W with an intact, fresh boronisation and thus higher $H_{98(y,2)}$ are most relevant as the boron-coated main chamber walls in AUG-W together with the tungsten divertor (typically not affected during a boronisation process) simulate more closely the situation in ITER of a Be main-chamber-wall and a tungsten divertor. In the experiments at AUG however, very large (giant) type I ELMs occurred, which appear difficult to mitigate at $q_{95} \sim 3$.

With the carbon wall in JET, baseline ELMy H-mode plasmas ($q_{95} = 3 – 3.6$, $\beta_N \sim 1.2 – 1.6$) achieved good normalised confinement with $H_{98(y,2)} \sim 1$ in unfuelled plasmas and only high triangularity plasmas could be fuelled up to the Greenwald density without reducing $H_{98(y,2)}$. In experiments during 2012 with the ILW, gas fuelling is required to avoid W contamination [39]. The low triangularity plasmas showed a similar degradation due to the fuelling as in JET-C. However, the good confinement in JET-C for the high triangularity plasmas could not be sustained in JET-ILW at high gas levels; a 20 – 30 % reduction in pedestal and, through profile stiffness, core confinement was observed. The confinement improves at higher beta values ($\beta_N \geq 2$) such that the hybrid scenario at JET shows no difference in overall confinement compared to carbon wall results [40].

Experiments in AUG and JET [39] with nitrogen gas puffing and AUG [36] with nitrogen and CH4 puffing show the pedestal can return to the higher level seen with the graphite wall despite enhanced radiation. At AUG, first attempts using nitrogen seeding in the ITER demonstration discharges (1.1 MA) were done at high β_N values (~2.5). At such high β_N energy confinement ($H_{98(y,2)}$ up to 1.15) clearly improved with the injection of nitrogen.

One common theme from these experiments is that is it difficult to obtain stable, stationary conditions when the loss power is just above the power threshold for entering H mode. Results for Alcator C-Mod are shown in Figure 10. The primary effect is that the ELMs become infrequent, leading to a rise in the electron density and, in devices with metal walls, a rise in the impurity density and core radiation.

Confinement is often seen to degrade as the density approaches the empirical density limit. In Alcator C-Mod using ICRF heating, flattop plasmas targeting ITER baseline parameters have been sustained for 20 τ_E or 8 – 13 τ_{CR}, but only reach $H_{98(y,2)} \sim 0.6$ at $f_{GW} = 0.85$, rising to 0.9 at $f_{GW} = 0.65$. Since the power threshold increases with density, it is difficult to separate the effects of the density limit from the effects of the loss power dropping near the power threshold. The scaling of the H-mode power threshold is uncertain, but the best estimates of P_{loss}/P_{LH} for baseline scenario in ITER are not significantly above 1. This will be discussed further in section V.

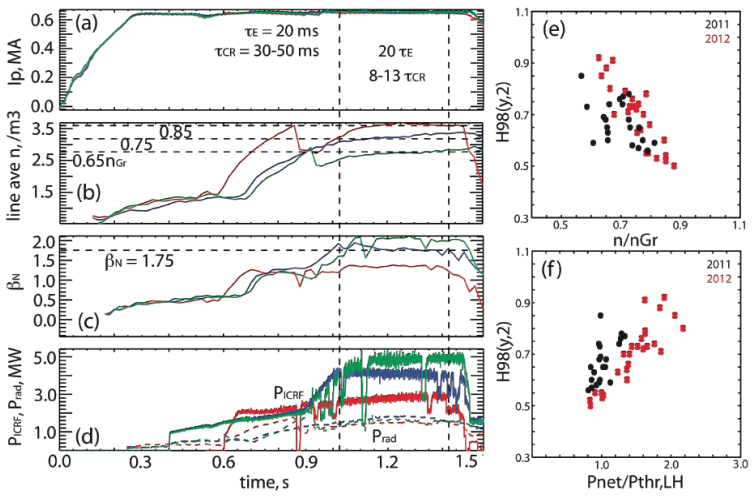

FIG. 10. *Stationary conditions are more difficult to achieve in Alcator C-Mod with $P_{in}/P_{LH} \sim 1$. Reproduced with permission from [C.E. Kessel et al, "Alcator C-Mod experiments in support of the ITER baseline 15 MA scenario", Nucl Fusion* ***53*** *(2013) 093021].*

The baseline scenario presents many challenges to the ITER design, especially the potential of off-normal events, because of the large free energy in the poloidal magnetic field. Reaching the primary physics objective at reduced plasma current would reduce many of the operational concerns. A brief discussion of the alternatives is given here; a more extensive review of the data and modelling is found in [2].

As noted in the opening paragraph, reaching the ITER Q = 10, 500 MW fusion power objective at lower current requires significant increases in the values of the pressure and confinement metrics. For example, at q_{95} = 4, β_N would need to increase to 2.4 and $H_{98(y,2)}$ would need to be 1.3. Likewise, at q_{95} = 5, β_N would need to increase to 3.0 and $H_{98(y,2)}$ would need to be 1.6. Over the last decade, inductive scenarios (mainly at q_{95} = 4) capable of higher normalized pressure ($\beta_N \geq 2.4$) than the ITER baseline scenario (β_N = 1.8) with normalized confinement at or above the standard H-mode scaling are well established under stationary conditions on the four largest diverted tokamaks (AUG, DIII-D, JET, JT-60U). A database of more than 500 plasmas from these tokamaks has been analysed [2], showing that the parameter range for which high performance is achieved is broad; both in q_{95} (see Figure 11) and density normalized to the empirical density limit.

Although some uncertainty remains, it appears that the stationary current profile, with q(0) near 1 but with flat magnetic shear in the centre observed at $q_{95} \sim 4 - 5$ and $\beta_N \sim 2.5 - 3.5$ yields both improved stability to tearing modes and improved confinement. The key point is that defining the access conditions for entering this stationary state is critical to achieving this type of operation in ITER. In addition to opening the operating space, the reduced plasma current and increased β_N lead to the possibility of much longer pulse operation in ITER, due

to the reduced flux required to supply the inductive magnetic energy, the higher temperature reducing the resistivity, and the increased bootstrap current. With suitable auxiliary equipment, ITER might be capable of high Q operation approaching an hour in duration.

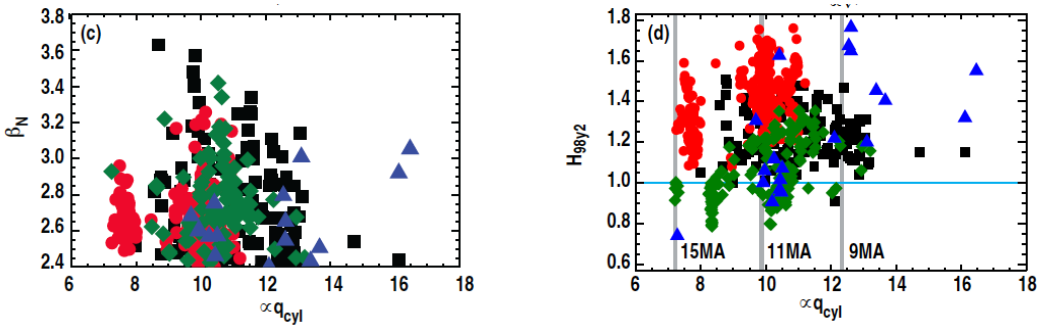

FIG. 11. *Advanced inductive plasmas achieve stationary high performance across a broad range of q_{95} in present-day tokamaks. Reproduced with permission from [T.C. Luce et al, "Development of advanced inductive scenarios for ITER", Nucl. Fusion* ***54*** *(2014) 013015].*

IV. Progress in scenario modelling

A. ITER baseline operating space

The poloidal field coil system on ITER is a critical element for achieving mission performance. Analysis of PF capabilities has focused on the operating space available for the 15 MA Q = 10 scenario. The flux consumption of the scenario is important, as ITER will operate close to the limitations of the power supplies and magnetic coil systems, with a maximum flux swing of ~ 240 – 265 Wb depending on the details of the PF coil settings.

Simulations have encompassed plasma initiation, current rampup, plasma burn and current rampdown, and have included density profiles and thermal transport models producing

temperature profiles consistent with edge pedestal conditions present in present day experiments. The simulations have been performed using three free-boundary transport simulation codes, TRANSP/TCS [58], CORSICA [47] and DINA. The simulations use a prescribed density profile evolution and the Coppi-Tang [41] thermal transport model to evolve the plasma for the baseline 15 MA inductive scenario.

Prior to the rampup phase, the plasma will be initiated followed by an early startup phase, where about 20 Wb are used to raise the voltage in the plasma region to its maximum, produce the plasma, form the current channel and bring the plasma current up to ~ 0.5 MA, taking approximately 1.5 s. The plasma has a large bore cross-section, roughly circular or slightly elongated, and limited on the inboard (or outboard) midplane walls. About 15 s into the current rise from 0.5 to 15 MA, corresponding to ~ 4 MA, the plasma is diverted to a lower single null configuration, and low power levels (5 – 10 MW) can be injected to heat the plasma.

The entire rampup from 0.5 to 15 MA, with additional heating, can require between 190 and 225 Wb depending on a number of features such as the energy confinement, heating level and heating type, whether an H-mode is induced, and the rampup time. Since an ohmic rampup over 100 s would require about 250 Wb, in general, it is necessary to heat the plasma in the rampup in order to guarantee flux is available for the flattop burn duration, although levels of 5 – 20 MW are sufficient with reasonable assumptions for energy confinement. In ITER, ECH provides direct electron heating and is most effective, although ICRF is also sufficient for this purpose. NB heating can only be injected above a minimum density in order to avoid shine-through heating of the wall components, and so it is normally reserved for the high

heating phase when entering the H-mode, either late in the rampup or at the end of the rampup.

The flattop phase requires 30 – 40 Wb to sustain the high temperature plasma for ≥ 300 s. In the rampdown phase the plasma current will be ramped from 15 MA down to about 10 – 15 % of this value. The duration of this phase could range from 100 to 200 s. The density is reduced during the rampdown phase, keeping the line-averaged value at 0.85 of the Greenwald density, with the profile shape preserved, corresponding to $n(0)/\langle n \rangle = 1.05$ (where <> denotes the volume averaged value). For this density profile, $n(0) \sim \langle n \rangle \sim n_{ped}$, although variations of this have not been found to significantly affect the scenario simulation. The pedestal is removed when the plasma transitions to L-mode, which occurs in the simulations when the input power drops below the L-H threshold power. The density profile then switches to a more peaked shape with $n(0)/\langle n \rangle \sim 2.0$, while the temperature profile preserves its core shape, but with the pedestal removed, giving $T(0)/\langle T \rangle \sim 3.0 – 3.5$. The CS coils will be near their current/field limits at the end of the flattop phase, and therefore should only decrease in current during the rampdown phase. Simulations indicate an over-current of the central solenoid coils if the plasma transitions from H to L-mode at the end of the flattop phase, due to the sudden inward motion of the plasma. Maintaining the plasma in H-mode when entering the rampdown phase and sustaining it sufficiently long (roughly 1/3 to 2/3 into the rampdown) avoids this response in the central solenoid coils. This also has the benefit of improving vertical stability, at least temporarily, due to a slowing in the rise of l_i (peaking of the current profile). These simulations to develop a viable rampdown scenario have been validated experimentally (section III.B).

The time-dependent simulations have been performed, with target coils current guided by parameter variations in static equilibria. These simulations represent the present state-of-the-art in producing scenarios representative of experimental conditions. These simulations show that the requirements for the PF coils are consistent with the operating space boundaries set by maximum allowed coil currents and forces. The results for 15 MA are summarised in Figure 12 [42].

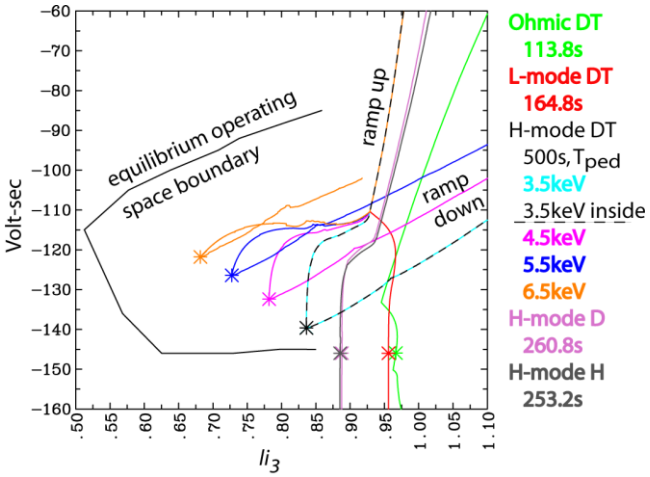

FIG. 12. *Mapping of the operating space in ITER with the various different assumptions for the current rise phase and edge pedestal temperature for the flat top phase. Simulations of ohmic and L-mode plasmas reach the coil limits after 114 s and 165 s respectively. Higher pedestal temperatures for DT plasmas give lower plasma inductance during the flat top phase. H-mode in deuterium reaches the coil limits after 261 s. Reproduced with permission from [T. Casper et al, "Development of the ITER Baseline Inductive Scenario", Proc. 23rd Int. Conf. on Fusion Energy, Daejeon, Rep. of Korea, 2010 (Vienna, IAEA) (2010) ITR/P1-19].*

Static equilibrium analyses for the baseline scenario for the various phases of the discharge has motivated an optimisation of the originally proposed PF coil system to allow low l_i (< 0.8) operation or plasmas with lower flux consumption. Moreover, the analysis also examined the feedback current reserve required in the central solenoid and PF coils during a series of disturbances, heating and current drive sources for saving volt-seconds in rampup,

flattop and the rampdown phase of the discharge. The vertical position and shape are controlled with the VS1 circuit that uses only the outer PF coils for control and the CS coils for ohmic current drive. Maximum current ramp rates, 50 s rampup and 60 s rampdown times, are limited only by the voltage capabilities of the power supply systems and not by vertical stability.

B. Long pulse operation at high plasma current in ITER

Simulation of ITER at 13 – 15 MA for a range of plasma densities ($<n_e>/n_{GW}$ = 0.5 – 1.0) [43] take into account the predicted values of the separatrix temperatures and densities, T_s, n_s, by the SOLPS code [44], including the effect of saturation of the plasma density associated with the onset of intense plasma recombination at the inner divertor. For ITER, SOLPS predictions for high power/high density scenarios required for fusion energy production, indicate that neutral penetration into the core plasma is negligible, breaking the link between separatrix density (controlled by gas puffing for divertor load control) and pedestal density (n_{ped}, controlled by pellet fuelling) [45]. These effects become more important at lower main plasma density ($<n_e>/n_{GW}$ ~ 0.5) for the separatrix values expected from SOLPS. EPED1 [46] predicts 30 % higher pedestal temperatures than with the standard assumptions of T_s = 75 eV and n_s/n_{ped} = ¼ (appropriate when recycled neutrals provide the main particle source in the core plasma). This higher electron temperature increases the NB and EC driven currents and reduces the resistive loss, thus allowing longer pulse operation in these conditions than for the reference 15 MA at Q = 10. The effect of the increased pedestal temperature on the burn length and on the achievable Q in this 15 MA low density scenario depends on the core plasma energy transport model. The largest effects are found for very stiff transport models (e.g. GLF23 [59]).

Several different codes have provided simulations for long pulse operation [43 and references therein]: JINTRAC [48] (using a BgB or GLF23 transport model), TOPICS [57] (using CDBM) and ASTRA (using a SBM, Weiland or MMM7.1 model). The various transport models used in the codes yield predictions of burn duration that are in reasonable agreement, as shown in Figure 13. The simulations show that long pulse operation in ITER (> 1000 s) can be achieved at 13 – 15 MA at reduced plasma density; the pulse length increases and the Q drops down to 5 (both for n_e reduction and I_p reduction). These types of discharges could increase the neutron fluence for TBM tests.

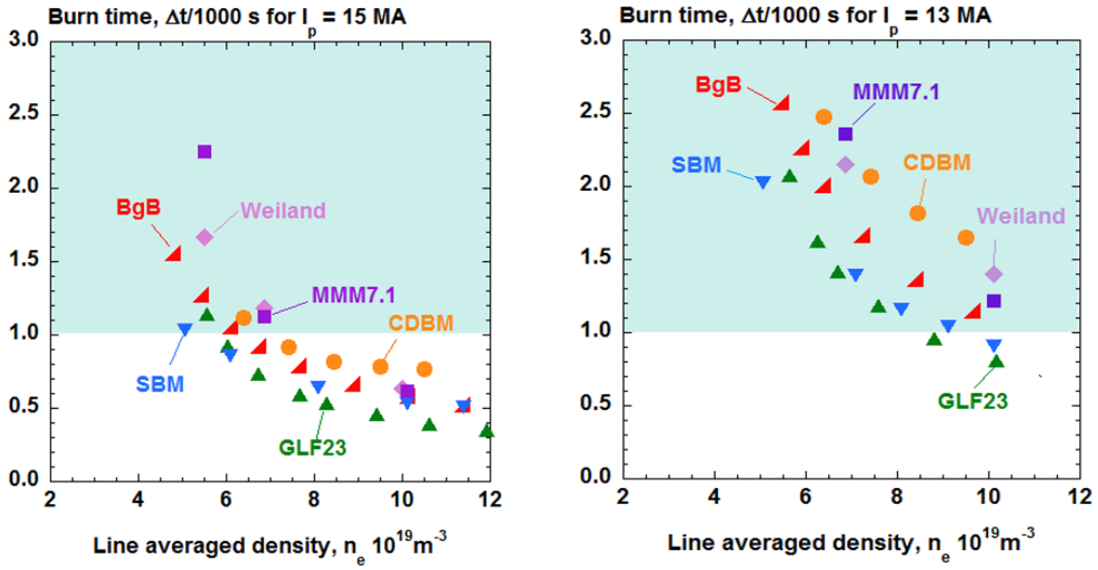

FIG. 13. *Simulations of the ITER flattop pulse length as function of the average plasma density. Various codes have provided simulations at 15 MA (left figure) and 13 MA (right figure) with good agreement of the results obtained. At 13 MA an increase in pulse length up to 2500 s is possible at lower plasma density. Reproduced with permission from [A.R. Polevoi et al, "Optimisation of ITER Operational Space for Long-pulse Scenarios", 40th EPS Conference on Plasma Physics, Espoo, Finland (2013) P2.135].*

C. Non-active operation

A non-active phase of operation is planned for the first few years of operation in ITER. For hydrogen operation in ITER the maximum input power will be in the range 53 – 63 MW, depending on the use of the ^{3}He minority ICRF heating scenario. For helium operation 63 MW will be available. To limit the NBI shine-through power to the first wall to below 4 MW/m^2, the minimum density to avoid excessive NBI shine-through in ITER has been calculated. For 100 % hydrogen this would be 4.5 x 10^{19} m^{-3} (already at 80 % of the Greenwald density limit at 7.5 MA), although this would reduce to 3 x 10^{19} m^{-3} for Z_{eff} ~ 2 (e.g. 1 % neon). In 100 % helium, the density limit for NBI shine-through is 2.5 x 10^{19} m^{-3}. The NBI system can provide heating at all toroidal field values, provided the density is maintained above the minimum shine-through density. The EC system can provide central heating ($\rho < 0.4$) for B_t = 2 – 2.65 T using 2nd harmonic X-mode heating and for $B_t > 4.5$ T using for fundamental O-mode launch. ICRH can be used in helium plasmas at $B_t > 2.3$ T to provide central heating (using different frequencies), while for hydrogen operation, without ^{3}He, ICRF can only be used at $B_t > 3.4$ T in ITER.

Resonant Magnetic Perturbation (RMP) coils and ELM pellet pacing should be commissioned for the mitigation of heat loads to the divertor, but they may also be required for the control of W accumulation in H-mode plasmas. Although hydrogen operation would allow independent density control with pellets and gas and therefore be more representative of operation in deuterium or DT mixtures, access to H-modes may not be possible with only 53 MW of input power available, even at 2.65 T. As a result, the ITER Research Plan envisages using helium plasmas to provide experience with H-mode operation. Operation in helium at high density however is uncertain due to limitations of having only gas fuelling available (requiring a particle pinch to provide core fuelling) and due to a low divertor detachment limit in helium. ELM pacing in helium H-modes by the hydrogen pellets can lead

to substantial dilution and potential loss of H-mode. Moreover, experiments show that H-modes in helium are very different from H-modes in deuterium, although a variety of different results have been obtained: AUG observes that ELMs in helium are much smaller and do not lead to W accumulation, while in C-Mod only ELM free H-modes are observed in helium (no EDA), and substantial Mo radiation typically results in a radiative collapse.

In preparation for operation in hydrogen and helium, several simulations have been performed with CORSICA [47] and JINTRAC [48]. The time-dependent simulations were performed for reduced operation at 7.5 MA and 2.65 T as well as at 15 MA and 5.3 T. Key in these simulations is the access to H-mode, without the α-heating from DT reactions. In the predictive simulations, the L-H transition threshold power is given by the standard scaling [49] without hysteresis. An inverse species mass scaling based on experimental results [50] is used for hydrogenic species. CORSICA assumes the same L-H threshold power scaling for both D and He while the JINTRAC work assumes the more pessimistic scaling for He that is 40 % above the D results. In these simulations for the non-active scenarios in ITER, the temperatures for ions and electrons at the separatrix were set to 220 eV and. 170 eV respectively. During H-mode, the pedestal is at $\rho \sim 0.92$. The plasma is assumed to be in type-III ELMy H-mode, if $P_{net} = (P_{tot} - dW_{th}/dt)$ is between P_{L-H} and 1.4 x P_{L-H} and in type-I ELMy H-mode for $P_{net} > 1.4 \times P_{L-H}$ (where W_{th} is the thermal stored energy of the plasma, P_{L-H} the power required to transition from L- to H-mode).

Simulations for hydrogen at 15 MA and 5.3 T with a maximum of 63 MW (assuming an ICRF heating scheme can be used) heating power, remain in L-mode even at the lower prescribed L-mode density of $\langle n_e \rangle = 0.5 n_{GW}$. Moreover, after only 20 s of flat top at 15 MA the central solenoid current limit is reached. In JINTRAC, the auxiliary heating was

optimised indicating the possibility of a flat top in L-mode > 50 s. Helium plasmas at 15 MA, 5.3 T may obtain a dithering H-mode at maximum input power with brief H-mode phases dropping back to L-mode due to the density rise during the H-mode phase. So, given the nominally available heating power of 63 MW, it is unlikely that ITER can achieve robust H-mode operation in hydrogen or helium at 5.3 T.

At 7.5 MA and 2.65 T, the required heating power in hydrogen at low plasma density ($0.5n_{GW}$) is close to the L-H threshold power and a small reduction in the available power will drop the plasma into a poor quality H-mode. For hydrogen, at 7.5 MA 2.65 T H, only type-III ELMy H-mode is reached with $T_{i,ped}$ ~ 1500 eV and $T_{e,ped}$ ~ 1400 eV. This implies that the nominal auxiliary heating power available is at best marginal for hydrogen operation at 2.65 T. The simulations show that there is no limit to the CS coils or PF coils for a flat top length of 200 s at 7.5 MA (even in L-mode). The simulation results for hydrogen and helium at 2.65 T are given in Figure 14. For helium operation, H-mode may be possible down to a power level of 35 MW suggesting sufficient margin for H-mode operation, at 7.5 MA, 2.65 T the plasma is predicted to reach good type-I ELMy H-mode conditions with $T_{i,ped}$ ~ 3700 eV, $T_{e,ped}$ ~ 3500 eV. Using JINTRAC, predictions for helium operation at 7.5 MA and 2.65 T have been optimised showing that the flat top could be extended beyond 300 s. Hence, ITER has a good probability of reaching H-mode operation in helium at half field and current with the nominal power available, without limitations posed by the poloidal field coils

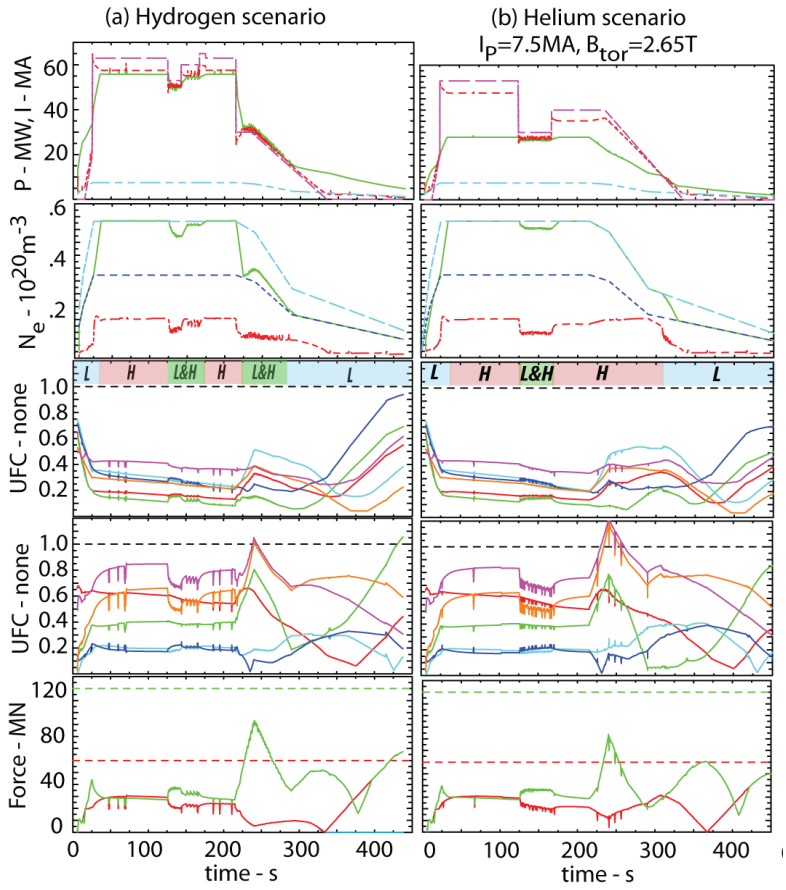

FIG. 14. *CORSICA simulations of (a) H and (b) He scenarios at half current (7.5 MA) and half magnetic field (2.65 T) for ITER; From top to bottom the panels show the input power compared to the L to H threshold power, on-axis density and temperature, The "coil utilisation factor" (UFC) is the "distance" from the coil limits (1.0 being the limit) for CS and PF coils and the coil forces. The period of L-mode and H-mode are indicated. Reproduced with permission from [T. Casper et al, "Development of ITER scenarios for pre-DT operations", Proc. 24th Int. Conf. on Fusion Energy, San Diego, USA, 2012 (Vienna, IAEA) (2012) ITR/P1-15].*

D. Benchmarking hybrid and steady-state simulations

Prediction of the detailed characteristics of the main ITER scenarios are based on a number of integrated modelling suites of codes. These are complex combinations of modules that compute, at various levels of approximation, the time evolution of magnetic equilibria,

density, temperature, and current profiles (sometimes also rotation and impurities), together with the appropriate transport coefficients, as well as source and loss terms. The latter are usually the most sophisticated and time consuming part of the computations. For instance, NBI modules can be based on Monte-Carlo codes and RF modules on wave propagation codes (ray-tracing or full wave) combined with 3-D Fokker-Planck codes. In view of this complexity, agreement of the results of various suites of codes, although including the same physics and using similar approximations and numerical methods, are by no means guaranteed. In the future, the need for detailed ITER scenario calculations is expected to increase; simulations of segments of discharges will also be used as a basis for preparing machine operation. This considerable amount of work should be on one hand based on a sound common ground and on the other possibly shared among various codes and groups of the ITER partners. For these reasons, a benchmark of the main integrated modelling suites of codes is considered an important preliminary step on which ITER scenario predictions should be based.

Benchmark activities have been performed in the framework of the ITPA-IOS group since 2005. Five 1.5D transport evolution codes (including either fixed or free-boundary equilibrium computation) have been involved in simulations for ITER: ASTRA [51], [52], CRONOS [53], ONETWO [54], FASTRAN [55], TOPICS-IB [56], [57] and TSC/TRANSP [58]. Initially, a set of parameters of an ITER hybrid scenario and the heat transport model GLF23 [59], have been chosen. Simulations have been performed limited to the evolution of current and temperatures (i.e., with non-evolving density, rotation and impurity profiles). This benchmark exercise was extended to steady-state scenarios [6], one characterised by high pedestal and weak shear, and a second study with ITB. The results of the benchmarks for the hybrid and steady-state scenarios are summarized here.

D.1 Hybrid scenarios

The benchmark exercise [5] has been performed for an ITER hybrid scenario characterized by a plasma current I_p = 12 MA, a flat electron density profile with central value $n_e(0) = 0.85 \times 10^{20}$ m^{-3}. An overview of the parameters obtained is given in Table 1. For these simulations the pedestal parameters are specified as $\rho_{ped} = 0.925$, $n_{ped} = n(\rho = 0.925) = n(0) = 0.85 \times 10^{20}$ m^{-3}, T_{ped} is set to 5 keV. The D-T fuel ion ratio is assumed to be 50 – 50 %. The impurities are Be and argon (Ar), with assumed fractions of 2 % and 0.12 %, respectively. The impurity density profiles are forced to be the same as the electron density, while the impurity temperatures are set equal to the main ion temperatures. The fuel ion density profiles are determined from quasi-neutrality. The injected powers are limited to the negative ion NBI (1 MeV, 33 MW, steered to full off-axis) and ICRF heating (20 MW, 53 MHz, 2nd T harmonic).

The main goal of this exercise was to compare the outputs of the codes and to identify possible sources of disagreement. The five codes globally provide a similar description of the main properties of the scenario. As shown in Table 1, the confinement enhancement factor ranges from 1.07 to 1.23, with normalised beta from 2.1 to 2.4 giving a range for the prediction of the fusion gain of 6.5 – 8.3. Nevertheless, substantial differences were observed in the heat sources profiles (α-power, NBI and ICRH), as well as in the implementation of the GLF23 heat transport model (use of pressure stabilization term, rotation stabilization features, and approaches used to stabilize the algorithm). In addition, there are still some discrepancies in the computed radiation losses for the hybrid simulations (including a possible over/under counting of bremsstrahlung and line radiation) that need to be resolved.

Table 1. *Scalar parameters for the benchmarking of the hybrid scenario at 12 MA, 5.3 T, using the GLF23 transport model in five different scenarios codes. The central electron and ion temperatures are given, together with the non-inductive current contributions from NB, EC and the bootstrap current giving a total non-inductive fraction (f_{NI}). P_α represents the fusion generated α-power and q(0) the central value of the q-profile* in stationary conditions. *Reproduced with permission from [C.E. Kessel et al, "Simulation of the hybrid and steady state advanced operating modes in ITER", Nucl. Fusion **47** (2007) 1274]*.

	ONETWO	TOPICS	TSC/TRANSP	CRONOS	ASTRA
$T_e(0)$ (keV)	27.2	31	33.8	26.3	33.5
$T_i(0)$ (keV)	33.4	32.3	33.8	25.6	32.3
I_{BS} (MA)	3.87	3.83	3.39	4.26	2.89
I_{NB} (MA)	2.07	2.26	1.42	0.92	1.91
I_{EC} (MA)	-	-	-	-	-
f_{NI}	0.50	0.51	0.40	0.43	0.40
Q	6.5	7.7	7.5	8.3	7.9
P_α (MW)	69	82	80	87.6	83.3
β_N	2.1	2.38	2.18	2.3	2.07
$H_{98(y,2)}$	1.1	1.07	1.18	1.23	1.2
q(0)	0.58	0.50	0.44	0.69	0.43

Therefore, a second step was undertaken, imposing strict guidelines in the benchmark. In order to discriminate the differences originating from the transport solvers from those associated with the heating sources, two additional test cases were defined, still on the basis of the previously used parameters [5]: 1) a test case with analytically prescribed heating and CD sources (to check the temperature and current profile evolutions and the transport coefficients); 2) a test case with analytically prescribed temperatures (to check the computations of the heating sources). Four codes have participated in this benchmark [60]: ASTRA, CRONOS, TOPICS-IB and TSC/TRANSP.

The main results of test case #1 (prescribed heating and current drive sources) are shown in Figure 15. It appears that, although the four codes use the same transport model (GLF23), differences in its implementation and smoothing procedure cause quantitative differences of the heat diffusivities, which are eventually amplified in the time evolution (since the model depends on the temperature gradients). This causes in turn different final temperature profiles, in particular in the centre, therefore with little impact on the global energy content. The total and bootstrap current density profiles show a satisfactory agreement, which means that the implementations of the neoclassical coefficients in the codes are substantially equivalent. Differences of the q values in the pedestal and edge region are mainly due to differences in the geometry and magnetic equilibrium.

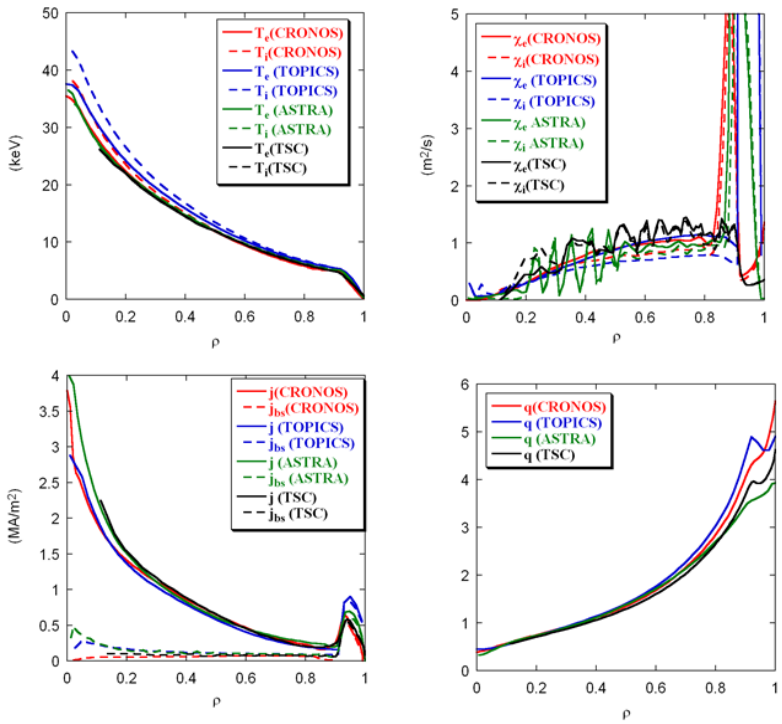

FIG. 15. *Hybrid scenario, Test case #1: comparison of temperatures (top left), heat diffusivities (top right), total and bootstrap current densities (bottom left), safety factors (bottom right) computed by different codes. Reproduced with permission from [G. Giruzzi et al, "Integrated modeling of steady-state scenarios for ITER: physics and computational challenges", Proc. 22nd Int. Conf. on Fusion Energy, Geneva, Switzerland, 2008 (Vienna,*

IAEA) (2008), IT/P6-4].

The profiles of the α-heating and NBI heating sources for the test case #2 (prescribed temperature profiles) are shown in Figure 16 (top panels). It has been found that differences in the α-heating profiles are mainly due to the different helium transport models used by the codes. In the bottom panels, the NBI, total and bootstrap current density profiles are shown. These figures show that, although the profiles are very similar, substantial differences in the NBI current drive efficiencies are still present and should be further investigated. In fact, the NBI deposition profiles have been the object of a separate benchmark exercise on NBI codes [61], [62], not summarised in this review.

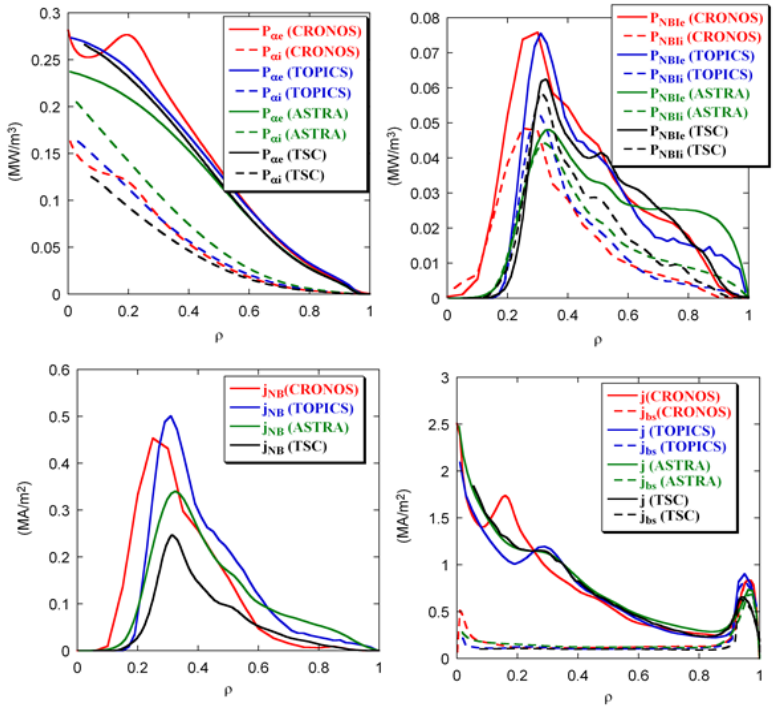

FIG. 16. *Hybrid scenario, Test case #2: comparison of alpha power depositions on ions and electrons (top left), NBI power depositions (top right), NBI driven current densities (bottom left), total and bootstrap current densities (bottom right) computed by different codes. Reproduced with permission from [G. Giruzzi et al, "Integrated modeling of steady-state scenarios for ITER: physics and computational challenges", Proc. 22nd Int. Conf. on Fusion Energy, Geneva, Switzerland, 2008 (Vienna, IAEA) (2008), IT/P6-4].*

D.2 Steady-state scenarios

A weak shear, high pedestal temperature steady-state scenario [6] has been analysed, characterized by I_p = 8 MA, a = 1.85m, a flat electron density profile with central value $n_e(0)$ = 0.65 x 10^{20} m^{-3} (which is at 110 % of the Greenwald density limit), and a pedestal temperature T_{ped} ~ 7 keV. The injected powers are the ITER day-1 systems: NBI (1 MeV, 33 MW, two NB injectors steered to full off-axis), ICRF heating (20 MW, 53 MHz, 90° phasing) and EC heating and current drive (170 GHz, 20 MW, equatorial launch steered for off-axis current drive (poloidal steering angle $\alpha = 0^o$ and toroidal steering angle $\beta = 35^o$). The GLF23 model was used with E *x* B shear multiplier of 1.0.

Table 2 shows the comparison of the global parameters calculated by six different scenario codes, showing good agreement. It was found that the overall results from different codes using the stiff theory-based (GLF23) model agree well [6]. There are still some discrepancies in the fusion products and, as mentioned before, differences in the computed loss mechanism (such as radiation). Global and local current balance is important for steady state scenarios. The total current densities are in excellent agreement, with some differences in edge current (mainly determined by the bootstrap contribution), resulting in differences in the edge-profile. The confinement enhancement factor ranges from 1.3 to 1.5, with normalised beta from 2.3 to 2.8 giving a range for the prediction of the fusion gain of 3.3 – 3.8.

Table 2. *Scalar parameters for the benchmarking of the weak-shear, steady state scenario at 8 MA, 5.3 T, using the GLF23 transport model in five different scenarios codes. The central electron and ion temperatures are given, together with the non-inductive current contributions from NB, EC and the bootstrap current giving a total non-inductive fraction (f_{NI}).* P_α *represents*

the fusion generated α-power and q_{min} the minimum value of the q-profile in stationary conditions. *Reproduced with permission from [M. Murakami et al, "Integrated modelling of steady-state scenarios and heating and current drive mixes for ITER", Nucl. Fusion* ***51*** *(2011) 103006]*.

	FASTRAN	TOPICS	TRANSP	CRONOS	ASTRA
T_{e0} (keV)	22.9	22.3	23.5	20.0	22.7
T_{i0} (keV)	20.1	18.7	19.9	19.7	20.0
I_{BS} (MA)	5.00	4.23	4.40	4.60	4.12
I_{NB} (MA)	2.33	2.94	2.29	3.00	3.26
I_{EC} (MA)	0.80	0.68	0.87	0.60	0.60
f_{NI}	1.06	1.03	0.99	1.06	1.04
Q	3.31	3.26	3.31	3.80	3.34
P_{α} (MW)	48.0	47.6	48.90	55.0	49.2
β_N	2.75	2.63	2.60	2.30	2.70
$H_{98(y,2)}$	1.49	1.48	1.43	1.30	1.36
q_{min}	1.72	1.81	1.90	2.10	1.85

Code comparison in ITB steady-state scenarios has been found to be much more challenging. A steady-state scenario [63] characterized by an ITB at mid-radius, purely RF current drive and 75 % of bootstrap fraction, originally computed with CRONOS has been used as a first test case for three codes: CRONOS, ONETWO/FASTRAN and TOPIC-IB. In ITER, an ITB would be associated with negative magnetic shear since the rotational shear would not be large enough to influence the confinement. Here, control of the current density profile is essential, but this is quite complicated when the bootstrap current is dominant. A conceptual solution is to use ECCD to lock the ITB and hence the bootstrap current profile. In these simulations prescribed heat diffusivity has been used:

$$\chi_{\mathrm{i}}(\rho) = \chi_{\mathrm{e}}(\rho) = \chi_{\mathrm{i}}^{\mathrm{neo}} + 0.4 * \left(1 + 3\rho^2\right) * F(s) \qquad (1)$$

where $F(s)$ is a function of magnetic shear (s) that is 0 for s < 0. LHCD (12 MW) is added outside the ITB to keep loop voltage zero.

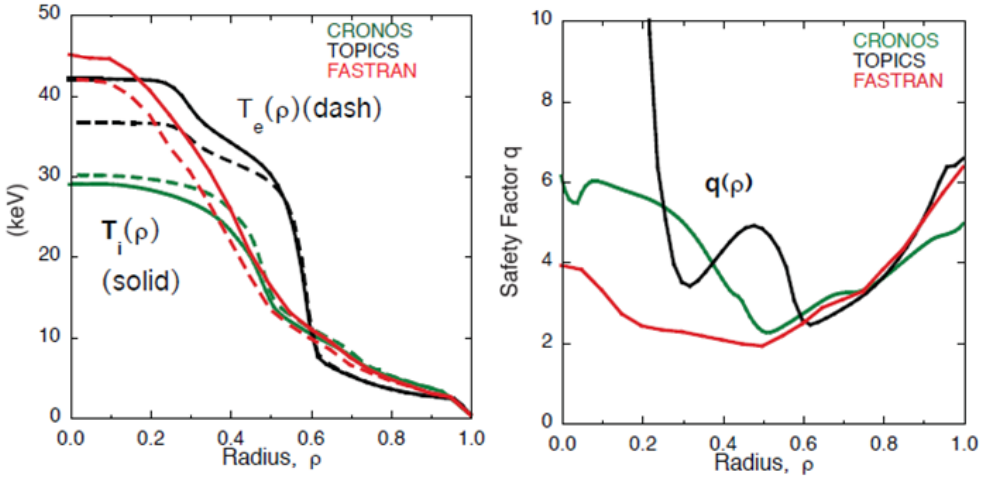

FIG. 17. *ITB steady-state scenario: comparison of electron and ion temperatures (left) and safety factors (right) computed by different codes. Reproduced with permission from [M. Murakami et al, "Integrated modelling of steady-state scenarios and heating and current drive mixes for ITER", Nucl. Fusion 51 (2011) 103006].*

Figure 17 shows that the resultant temperature and q profiles are very different for the three codes, because the strength of the ITB sensitively depends on the width and height of the ECCD profile, as well as from the bootstrap current profile, that peaks strongly at the ITB location. Further studies will be carried out on the issue of sustainability of the ITB by broadening the ECCD.

E. Advanced scenario explorations

Insight to the achievability of steady state operation in ITER has been obtained from simulating scenarios at reduced plasma current (7 MA – 10 MA) at 5.3 T. The ITER design

"should aim at demonstrating" fully non-inductive operation with a target of $Q \geq 5$. This implies that the pressure (profiles) and current (profile) must be stationary on a long timescale. A pulse length limit of 3000 s in ITER should be able to test these steady state scenarios. Assuming the use of high plasma density for power exhaust ($\langle n_e \rangle \sim 0.85\ n_{GW}$) the necessary plasma confinement for obtaining $Q \sim 5$ is in the range $H_{98(y,2)} = 1.3 - 1.7$. With simple estimates of the current drive efficiencies for neutral beam injection at 1 MeV and electron cyclotron heating available in ITER, the required bootstrap fraction for obtaining 100 % non-inductive operation varies from 50 % at 8 – 9 MA to 70 % at 11 MA, as shown in Figure 18 [64].

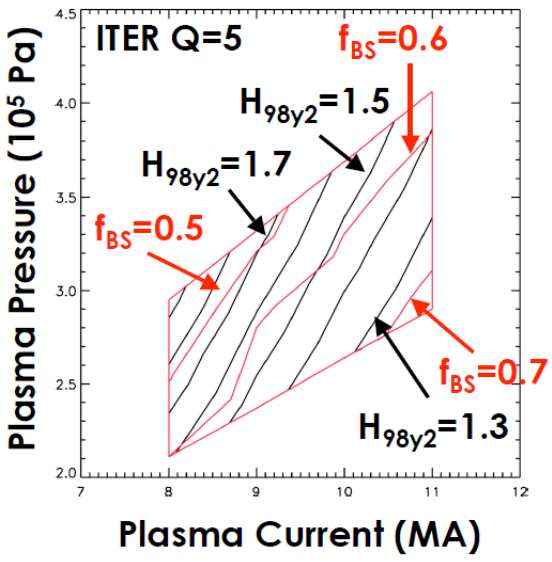

FIG. 18. *The operational space for non-inductive operation in ITER, At the pressure needed for Q ~ 5, the required $H_{98(y,2)}$ confinement factors are indicated by the black lines and numbers, while the required bootstrap fraction to obtain fully non-inductive operation with the current drive from NBI (33 MW) and EC (20 MW) are indicated by the red lines and numbers. Reproduced with permission from [T.C. Luce, "Reflections on ITER Steady-State Scenario Operational Space", Presented at the 1st Integrated Operational Scenarios Topical Group Meeting of the ITPA, 20 October 2008 (2008)].*

The high confinement required for steady state operation in ITER can be obtained by (1) operating at high edge pedestal pressure, with $T_{ped} \sim 7$ keV at 8 – 9 MA or (2) at lower edge pedestal pressure ($T_{ped} \sim 3$ keV) but with internal transport barriers (ITBs) at normalized pressures close to the ideal no-wall limits [65], [66].

Prediction of ITER steady state operation at 8 – 9 MA at high edge pedestal with a weak magnetic shear in the centre use a GLF23 transport model that is strongly affected by the boundary conditions. In the simulations, an edge-localized mode (ELM)-averaged edge profile scaled from that of an ITER steady state demonstration DIII-D discharge [67] was adopted near the boundary (ρ = 0.8 – 1.0). The operating current and field are I_p = 8 MA and B_T = 5.3 T. The top of the pedestal is set at ρ_{ped} = 0.91 with β_N = 1.20 at the top of the pedestal (resulting in the aforementioned T_{ped} = 7 keV).

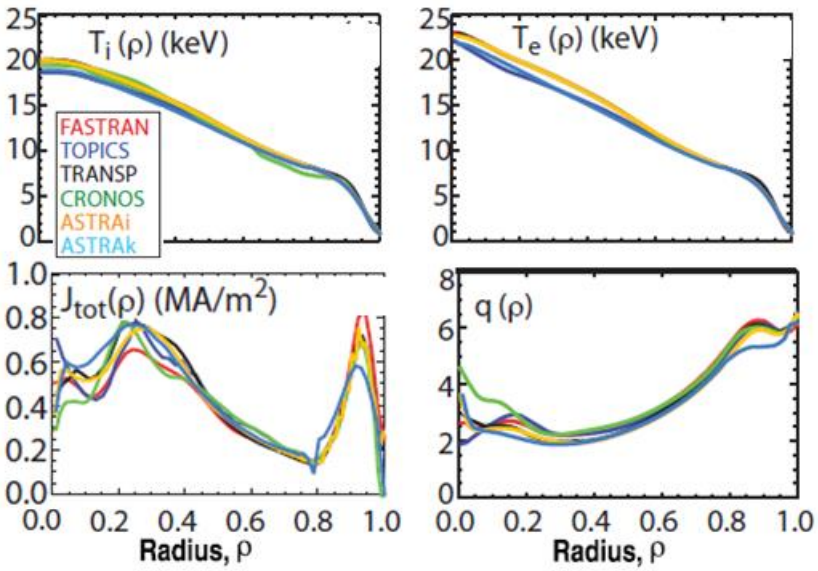

FIG. 19. *Weak shear steady-state scenario: comparison of ion temperatures (top left), electron temperatures (top right), current densities (bottom left), safety factors (bottom right) computed by different codes. Reproduced with permission from [M. Murakami et al, "Integrated modelling of steady-state scenarios and heating and current drive mixes for ITER", Nucl. Fusion 51 (2011) 103006].*

Figure 19 shows comparison of some kinetic profiles obtained from several simulation codes for this scenario. Note that two different implementations of the ASTRA code have been used. The q-profile (and low shear in the core) obtained is strongly determined by the edge

bootstrap current. Stability calculations show that with the assumptions made, the edge of the plasma is about 25 % above the peeling-ballooning stability limit calculated, which will be challenging to achieve in ITER. The effects of E *x* B stabilization on the profiles are small with less than 5 % (1 keV) difference in core temperatures for simulations with the stabilization terms switched on or off. Hence, the confinement is primarily determined by the magnetic shear.

By using the predictions for steady state operation in ITER using a weak-shear scenario the optimisation of the heating and current drive systems for ITER has been studied. For the day-1 reference H&CD mix shows that operation at higher I_p (e.g. 9 MA) would be important to reach Q ~ 5 objective. The high pedestal pressure provides bootstrap current at a level of 50 % – 60 % of the total plasma current. Neutral beam injection provides 2 – 3 MA of non-inductive current drive and ECCD provides a modest 0.6 – 0.9 MA.

Already introduced in section IV.D.2, a steady-state scenario characterized by an ITB at mid-radius, purely RF current driven and with 75 % of bootstrap fraction has been developed [63]. Extensive simulations have been performed with the CRONOS code studying ITB formation for ITER in reversed shear scenarios, using a model for the reduction of turbulent transport as given previously in equation (1). In these simulations, the pedestal temperature is fixed at $\rho \sim 0.93$ at a value of $T_{ped} \sim 3$ keV, which is a conservative value, with respect to the bootstrap current generated in the edge region. To avoid shrinking or erosion of the ITB, a method is needed to control the bootstrap current, which is in the core is dominated by the α-heating. The simulations show that the plasma forms a stationary ITB when EC is deposited at $\rho = 0.45$ at power levels 12 – 20 MW. The ECCD locks the ITB at mid-radius. Lower Hybrid current drive (13 MW) is located at $\rho = 0.7$ to provide a stable q-profile, contributing

to the total non-inductive current fraction. The parameters obtained for these 8 MA discharges are T_{e0} = 31 keV, T_{i0} = 30 keV, no NB current drive, I_{BS} = 5.6 MA, I_{EC} = 1.56 MA, I_{LH} = 0.6 MA, f_{NI} = 0.97, Q = 6.5, P_α = 70 MW, β_N = 2.8, $H_{98(y,2)}$ = 1.7 with q_{min} just above 2 and q(0) ~ 6.

The scenario described above places particular emphases on the ECH system being able to deliver sufficient current drive at mid-radius. For ITER the EC power is deposited at $\rho = 0.45$ by using a combination of power coming from the top-launchers and mid-plane launcher. The steering angles for these systems have been optimised recently as a direct result of these steady state scenario studies.

Several combinations of heating and current drive sources have been used in fully non-inductive scenario simulations for plasma currents in the range 7 – 10 MA [7]. Full plasma discharges are simulated with the Tokamak Simulation Code (TSC) [68] coupled with TRANSP [69] to provide models for the heating and current drive sources. A semi-empirical approach is adopted to produce an ITB in the electron and ion temperature through a modified thermal diffusivity profile: a combination of an L-mode Coppi – Tang model for the interior region and two terms to model, respectively, the ITB foot and the pedestal. The ITB foot location, ρ_{ITB}, is defined as the location of minimum thermal diffusivity. EPED1 predicts the pedestal temperature at $\rho_{ped} \sim 0.94$ to be in the range T_{ped} = 3.3 – 3.7 keV for I_P = 7 – 10 MA, and densities, $n(0) \sim (7.0 – 8.5) \times 10^{19}$ m^{-3} (with $n_{ped} \sim (4.0 – 5.0) \times 10^{19}$ m^{-3}). The thermal diffusivity profile is scaled to obtain $H_{98(y,2)} \sim 1.6$, while maintaining T_{ped} in the range predicted by EPED1. These simulations allow an assessment of the heating and current drive system requirements for non-inductive operation in ITER. In addition, ideal MHD stability has been analysed for variations of the Greenwald fraction and of the pressure

peaking factor around the operating point, aiming at defining an operational space for stable, steady-state operation at optimized performance.

It is found that 73 MW of heating power (20 MW IC and 20 MW EC combined with 33 MW NB), as planned for the initial operations on ITER, can sustain up to 7.4 MA of non-inductive current in the flat-top. This scenario has a fusion gain of Q = 2 – 3.5, operates at $\beta_N \leq 2.4$ and is predicted to be ideal MHD stable for variations of the plasma parameters around the operating point. Hence, this scenario (at low T_{ped} ~ 3 keV) would be therefore a good candidate to demonstrate the feasibility of steady-state, stable operations at moderate β_N, with densities close to the Greenwald density limit.

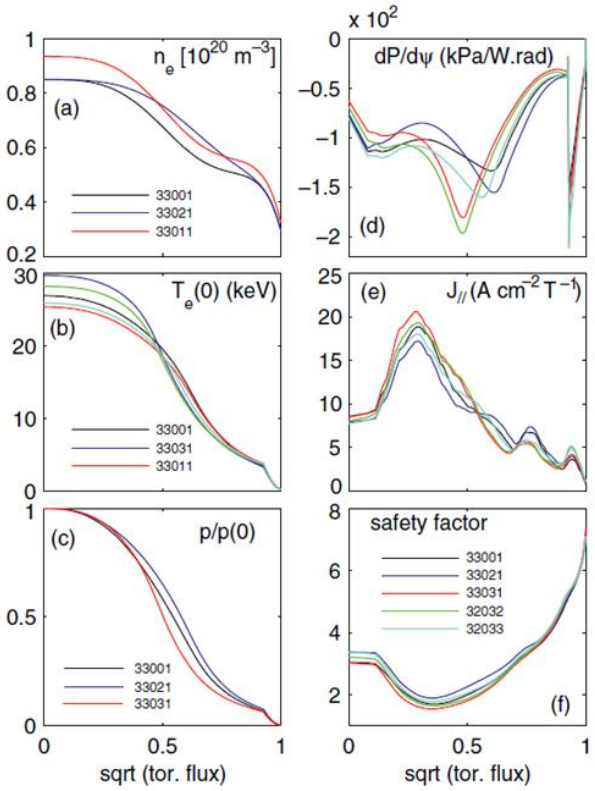

FIG. 20. *Scenarios with 20 MW EC, 20 MW LH and 33 MW of NB. (a) Density profiles for various cases of $n_e(0)/\langle n_e \rangle$. (b) Temperature profiles, (c) pressure profiles, normalized to the maximum, (d) pressure derivative, (e) total parallel current, (f) safety factor profiles. Simulation 33011 reaches Q = 5, β_N = 2.8 at I_p = 8.9 MA. Reproduced with permission from [F.M. Poli et al, "Ideal MHD stability and performance of ITER steady-state scenarios with ITBs", Nucl. Fusion* ***52*** *(2012) 063027].*

Different options are under consideration for upgrading the heating systems on ITER, including doubling the EC power to 40 MW or adding up to 40 MW of LH [70]. Using an

additional 20 MW of EC increases the non-inductive EC current to 1.5 MA with $Q \sim 3.4$ and $\beta_N \sim 2.4$ at 8.8 MA. As shown in Figure 20, a combination of 20 MW EC and LH has better performance with $Q = 5$ and minimum safety factor above 1.5.

V. Key Scenario Issues to Resolve for ITER Operation

As discussed in section III, the demonstration of the basic parameter regime for $Q = 10$ operation in ITER has been carried out in existing experiments. However, these experiments have some fundamental differences from the conditions expected in ITER. In this section, these differences are explored, pointing to limitations in the predictability of ITER performance and potential experiments that could address them prior to ITER operation.

Perhaps the highest leverage assumption in the projections to ITER is that of the width and height of the H-mode pedestal. A model (EPED1, [46]) based on the intersection of stability limits from ideal MHD theory and transport limits set by kinetic ballooning modes has had some success in describing the trends seen in experiments. For predictive purposes, it serves more as a limiting guideline rather than a definitive model, since it does not specify how to separate the pressure into density and temperature or divide it between the electrons and the ion species. The model describes existing pedestal pressure data within a band of about ± 20 %, but this could lead to ± 40 % change in the fusion power and perhaps even larger variations in the predicted gain. In addition, the pedestal current density plays a significant role in the overall current profile at ITER-relevant conditions, which in turn determines to a large extent the tearing stability of the plasma. The experimental approach to minimize the effect of the uncertainty in the pedestal behaviour has been to remove differences between the

existing experiments and ITER as much as possible, e.g., operating with a similar poloidal cross section. Dedicated experiments showing the sensitivity of the scenario to changes in the pedestal will help clarify where further work is needed.

As noted in section III, ITER is expected to have significantly lower rotation than existing experiments that use co-NBI as the dominant heating source. ITER at Q = 10 will have 2/3 of the heating power from fusion α particles, which impart no net torque. The NBI system in ITER can inject a maximum of ~ 30 N-m of torque, which is only an order of magnitude more than present day experiments while the moment of inertia increases by several orders of magnitude. The key question is whether low rotation affects the scaling itself or only the multiplier of the scaling. Experiments indicate that it is only the multiplier [71], but no experiments exist studying directly the scaling of ITER scenarios. These experiments are very challenging, but could be carried out on existing tokamaks. In addition to these considerations, predictions of the intrinsic rotation are highly uncertain [72], [73] and the slowing of rotation from any source due to the effects of non-axisymmetric magnetic fields from ELM mitigation techniques or intrinsic error fields are difficult to assess. Simulations of ITER scenarios have used a zero rotation case as a reference that is expected to be conservative.

Operation with metal walls leads to both constraints and advantages for scenario optimization. Retention of hydrogen isotopes is much reduced in a metal wall machine compared with the experience in graphite. This is essential for meeting the safety requirements for licensing in ITER. The low retention also reduces the demand on wall conditioning both after a vacuum opening and between plasmas, simplifying operations. It also facilitates variation and optimization of the deuterium-tritium mixture by varying the fuelling mix. Experiments in

TFTR and JET with tritium were complicated by the difficulties in controlling the mixture due to release of near-surface inventory of hydrogen species in the graphite tiles. On the other hand, the presence of tungsten raises concerns with impurity accumulation. The plasma incident on tungsten surfaces must be sufficiently low temperature to minimize sputtering. The plasma configuration must also minimize the uptake of sputtered tungsten into the core plasma because confinement of high-Z impurities is very good, due to strong inward neoclassical transport. Even though the main chamber is low-Z metal in ITER (beryllium), the preliminary experience in JET with the ITER-like wall shows that the change from graphite to beryllium has a strong effect on the pedestal behaviour that was not predicted prior to the experiments. Further experiments with the new wall in JET compared with the prior graphite experience and the significant variation in wall materials in other present-day tokamaks should shed light on how ITER may vary from the existing physics basis used to design ITER.

Related to the wall issues is the need to control the steady-state and transient heat fluxes to the divertor and main chamber walls. The ITER divertor is designed to take the steady-state power of the Q = 10 design scenario. Divertor operation is envisioned to include sufficient neutral deuterium and tritium gas source to distribute the heat more evenly by converting a substantial fraction of the thermal energy entering the divertor into radiation. In addition, some low-Z impurity such as neon or nitrogen may be introduced to enhance the radiation in the divertor and, if possible, in the main chamber. The main issue is the compatibility of this mode of operation to treat the steady-state heat flux with the high-performance core plasma required to reach Q = 10. As discussed in section III, the initial work on JET showed a strong degradation of global energy confinement with increased gas puffing. Similar effects are seen on other tokamaks, although the reduction in confinement is somewhat mitigated by strong

pumping to limit the recycling. Accumulation of the impurity added to enhance the radiation is seen, but the effect of this is not as large as with tungsten, because the impurities used will be fully ionized in the core and will not contribute strongly to either the power balance or fuel dilution. Radiation inside the plasma can reduce the power flow through the pedestal, which may already be marginal for sustaining stationary H-mode operation.

The impact of limiting the transient heat loads expected from ELMs may be more severe. ELMs have long been known to have a favourable effect on screening impurities, but the magnitude of a single ELM in ITER at q_{95} = 3 is predicted to be so large as to cause substantial deterioration of the material surfaces where the energy is deposited. The gas puffing discussed above for steady-state heat flux mitigation is also known to increase the ELM frequency with a corresponding decrease in magnitude of individual ELMs. However, this implies a reduction in the time-averaged pedestal pressure, which may be the source of the confinement reduction observed with gas puffing. Other methods of increasing the ELM frequency such as perturbations to the plasma boundary with vertical motions or initiating ELMs with pellets will have the same issues. In the other direction, methods to avoid ELMs by limiting the pedestal pressure with non-axisymmetric magnetic fields or axisymmetric shaping may also lead to a reduction in the global energy confinement. Few experiments (e.g. AUG [36]) have explored ELM mitigation at the q_{95} = 3 envisioned for the baseline Q = 10 scenario in ITER; there is clearly a need for more experiments to explore the coupled effects between the core and edge solutions. For scenarios at higher q_{95}, the ELMs are typically more frequent and smaller in magnitude, but it may be necessary to go as high as q_{95} = 5 to avoid the need for ELM mitigation for protection of the first wall material.

Finally, an area that is relatively unexplored is the need and development of control of the scenario in burning plasmas. The basic feedback control of shape, current, and density is highly developed in present-day experiments. Three critical areas of scenario control have been identified for ITER. Most critical is control of the exit from burn, both in planned and unplanned shutdown sequences. As discussed above, the interplay of the core and edge solutions is a delicate balance during the stationary burn, but the control of this is not likely to be very complex. What is more complex is sequencing the reduction of the plasma density, the heat flux mitigation method, and the fusion burn in such a way that the plasma is robustly stable to axisymmetric and non-axisymmetric instabilities during the current rampdown phase while sharing a limited set of actuators. This appears to be quite challenging even for planned shutdown, but will be even more challenging when an off-normal event requires an unplanned shutdown of the plasma burn. Exploring various trajectories in present-day experiments in order to define criteria sufficient for orderly shutdown is very important. Entry to burn also presents challenges not faced by present experiments. As discussed in section III, both the baseline scenario and the alternate approaches for Q = 10 operation must meet some (presently undefined) access criteria to avoid triggering tearing instabilities. In ITER, the relatively rapid onset of fusion power adds a complication not faced in present-day experiments. Simulations indicate that the ITER heating systems should have sufficient dynamic range to prevent both excessive overshoot of the pressure or a fizzle, but this needs to be verified in present-day experiments dedicating some heating systems to imitate the fusion power correlation with pressure. Control of the current rise may also be necessary to provide a current profile at the end of flattop that allows stable development of the scenario as the current relaxes resistively to equilibrium.

VI. Summary and Conclusions

In recent years, dedicated experiments and coordinated scenario simulations, initiated by the Integrated Operation Scenarios Topical Group of the ITPA, have significantly advanced the preparation of ITER operation. The experiments cover a wide range of topics such as plasma formation, plasma rampup and reliable rampdown, the demonstration of the ITER baseline and alternatives to achieve the ITER goal of Q = 10 at 500 MW of fusion power at Q = 10. Scenario simulations have been benchmarked and provide insight to the requirements for achieving long sustained burn, steady state operation and early operation in hydrogen and helium in ITER. This paper reviews the progress made.

The ITER Research Plan defines a success oriented schedule for ITER operation and exploitation. The initial operation phase of system commissioning and scenario development will be in hydrogen and helium. This will be followed by a nuclear operation phase starting with deuterium operation but proposing a rapid development (within 1 year) of deuterium-tritium operation towards a demonstration of Q ~ 10. Joint activities have been coordinated by the Integrated Operation Scenarios Topical Group of the ITPA to support the preparation of ITER operation in order to minimise the risk for the proposed research plan for ITER.

Plasma formation has been studied. Experiments with metal walls and in particular JET with a beryllium first wall, report robust plasma breakdown over a wide range of conditions. Experiments using an inclined EC launch angle to mimic the conditions in ITER report successful EC assist, albeit in some conditions requiring a doubling of the input power compared to a radial launch. Simulations of the plasma burn-through, validated on JET data,

that include models for plasma-wall interactions, predict that at least 4 MW of ECH assist would be required in ITER.

For H-modes at q_{95} ~ 3 many experiments have demonstrated operation at the scaled parameters for the ITER baseline scenario at $n_e/n_{GW} = 0.8 – 0.85$. Experiments at DIII-D with a carbon wall have performed ITER demonstration discharges in conditions close to ITER. Experiments at C-Mod, AUG and JET have obtained results with metal walls, controlling high-Z impurity accumulation with gas fuelling and central wave heating. Most experiments, however, obtain $H_{98(y,2)}$ ~ 1.0 and stable operation as long as β_N is above 2 (typically $2.0 < \beta_N < 2.2$).

Experiments have tested the proposed schemes for the rampup and rampdown phases of the ITER baseline at 15 MA. For the rampup, early X-point formation is required, to avoid overheating the first wall and to allow early auxiliary heating to reduce the flux consumption. A range of plasma internal inductance ($l_i(3)$) can be obtained from 0.65 to 1.0, with lowest values obtained in H-mode operation. For the rampdown, the plasma should stay diverted and maintain H-mode. A reduction of the elongation from 1.85 to 1.4 is important; especially for emergency shutdown scenarios where maintaining H-mode in the current decay may not be possible.

Since 2007, a new reference current rise has been developed for 15 MA operations in ITER, including a large bore initial plasma, early divertor transition, and low level heating in L-mode and a late H-mode onset for the current rise phase. All are compatible with the current ITER design for the PF coils.

Simulations show that long pulse operation in ITER (> 1000 s) can be achieved at 13 – 15 MA at reduced plasma density with n_e/n_{GW} ~ 0.5 at Q ~ 5 (reduced Q resulting both for n_e reduction and I_p reduction); these type of discharges could provide neutron fluence for TBM tests.

Operation during the low-activation phase requires high power (> 50 MW) and sufficient plasma density to allow NB injection, with limits for the line-averaged density of 4.5 x 10^{19} m^{-3} and 2.5 x 10^{19} m^{-3} for hydrogen and helium respectively. H-mode operation in helium would be possible at input powers above 35 MW at 2.65 T, for studying H-modes and ELM mitigation. In hydrogen, H-mode operation would be marginal, even at 2.65 T.

A benchmark study for scenario code simulations has been performed using detailed parameter descriptions for hybrid and steady state scenarios. Testing the complex suites of codes, consisting of tens of sometimes very sophisticated modules, has proved a very challenging and lengthy task. Nevertheless, the general basis of the modelling appears sound, with a substantial consistency among codes developed by different groups and, in most cases, independently. At least some sources of differences have been identified and, in some cases, solved.

For the hybrid scenario the code simulations give a range for Q = 6.5 – 8.3, using 30MW NBI and 20MW ICRH. For non-inductive operation at 7 – 9 MA the simulation results show more variation, depending on the assumption made for the pedestal, core transport and heating power used. At high edge pedestal pressure (T_{ped} ~ 7 keV) simulations obtain Q = 3.3 – 3.8 using 33 MW NB, 20 MW EC and 20 MW IC (day-1 heating set in ITER). While for simulations using a lower edge pedestal temperature (~ 3 keV) but improved core

confinement obtain Q = 5 – 6.5, when ECCD is concentrated at mid-radius and current drive in the outer half of the plasma (ECCD or LHCD at 20 MW) is added to maintain the $q \geq 1.5$ (or is some simulations $q \geq 2$) everywhere.

Finally, the IRP highlights several issues for scenario preparation for ITER to be addressed. The main limitations or uncertainties of the scenario studies presented here are the height of the edge pedestal in ITER which will have an important effect on ITER performance, the plasma rotation with low net-torque input, impurities from (high-Z) metal walls, limiting heat loads by using high radiation fractions and reducing transient heat loads from ELMs.

Experiments and simulations preparing for ITER operation should continue and include the requirements for controlling the plasma burn together with reliable termination of the burning plasma.

Acknowledgements

The authors wish to thank the ITER-IO, and in particular the EFDA contributors, the ASDEX-Upgrade team, the DIII-D team and the C-Mod team. The views and opinions expressed herein do not necessarily reflect those of the ITER Organization.

References

[1] M. Shimada, D.J. Campbell, V. Mukhovatov, M. Fujiwara, N. Kirneva, K. Lackner, M. Nagami, V.D. Pustovitov, N. Uckan, J. Wesley, "*Progress in ITER Physics basis"*, Nucl. Fusion **47** (2007)

[2] T.C. Luce, C.D. Challis, S. Ide, E. Joffrin, Y. Kamada, P.A. Politzer, J. Schweinzer, A.C.C. Sips, J. Stober, G. Giruzzi et al, "*Development of advanced inductive scenarios for ITER"*, Nucl. Fusion **54** (2014) 013015

[3] C.E. Kessel, D. Campbell, Y. Gribov, G. Saibene, G. Ambrosino, R.V. Budny, T. Casper, M. Cavinato, H. Fujieda, R. Hawryluk et al, "*Development of ITER 15 MA ELMy H-mode inductive scenario"*, Nucl Fusion **49** (2009) 085034

[4] T. Casper, D.J. Campbell, V. Chuyanov, Y. Gribov, T. Oikawa, A. Polevoi, J. Snipes, R. Budny, I. Voitsekhovitch, P. Bonoli, F. Koechl, and ITPA IOS, "*Development of ITER scenarios for pre-DT operations"*, Proc. 24th Int. Conf. on Fusion Energy, San Diego, USA, 2012 (Vienna, IAEA) (2012) ITR/P1-15

[5] C.E. Kessel, G. Giruzzi, A.C.C. Sips, R.V. Budny, J.F. Artaud, V. Basiuk, F. Imbeaux, E. Joffrin, M. Schneider, M. Murakami, T. Luce, H.E. St. John, T. Oikawa, N. Hayashi, T. Takizuka, T. Ozeki, Y.-S. Na, J.M. Park, J. Garcia and A.A. Tucillo, "*Simulation of the hybrid and steady state advanced operating modes in ITER"*, Nucl. Fusion **47** (2007) 1274

[6] M. Murakami, J.M. Park, G. Giruzzi, J. Garcia, P. Bonoli, R.V. Budny, E.J. Doyle, A. Fukuyama, N. Hayashi, M. Honda, A. Hubbard et al, "*Integrated modelling of steady-state scenarios and heating and current drive mixes for ITER"*, Nucl. Fusion **51** (2011) 103006

[7] F.M. Poli, C.E. Kessel, M.S. Chance, S.C. Jardin and J. Manickam, "*Ideal MHD stability and performance of ITER steady-state scenarios with ITBs"*, Nucl. Fusion **52** (2012) 063027

[8] D.J. Campbell, ITER Collaborators, "*Challenges in Burning Plasma Physics: the ITER Research Plan"*, Proc. 24th Int. Conf. on Fusion Energy, San Diego, USA, 2012 (Vienna, IAEA) (2012) ITR/P1-18.

[9] F. Ryter, T. Pütterich, M. Reich, A. Scarabosio, E. Wolfrum, R. Fischer, M. Gemisic Adamov, N. Hicks, B. Kurzan, C. Maggi, R. Neu, V. Rohde, G. Tardini and the ASDEX Upgrade TEAM, "*H-mode threshold and confinement in helium and deuterium in ASDEX Upgrade"*, Nucl. Fusion **49** (2009) 062003

[10] P. Gohil, T.E. Evans, M.E. Fenstermacher, J.R. Ferron, T.H. Osborne, J-M. Park, O. Schmitz, J.T. Scoville and E.A. Unterberg, "*L-H Transition studies on DIII-D to determine H-mode access for operational Scenarios in ITER"*, Nucl. Fusion **51** (2011) 103020

[11] D.C. McDonald, G. Calabrò, M. Beurskens, I. Day, E. de la Luna, T. Eich, N. Fedorczak, O. Ford, W. Fundamenski, C. Giroud, P. Gohil, M. Lennholm, J. Lonnroth, P.J. Lomas, G. P. Maddison, C. F. Maggi, I. Nunes, G. Saibene, R. Sartori, W. Studholme, E. Surrey, I. Voitsekhovitch, K-D. Zastrow and JET EFDA contributors, "*JET Helium-4 ELMy H-mode Studies"*, EFDA-JET Report (2010), EFDA – JET – CP(10)08/24

[12] J.A. Snipes, D.J. Campbell, P.S. Haynes, T.C. Hender, M. Hugon, P.J. Lomas, N.J. Lopes Cardozo, M.F.F. Nave and F.C. Schüller, "*Large amplitude quasi-stationary MHD modes in JET"*, Nucl. Fusion **28** (1988) 1085

[13] A.C.C. Sips, T.A. Casper, E.J. Doyle, G. Giruzzi, Y. Gribov, J. Hobirk, G.M.D. Hogeweij, L.D. Horton, A.E. Hubbard, I. Hutchinson et al, "*Experimental studies of ITER demonstration discharges"*, Nucl. Fusion **49** (2009) 085015

[14] B. Lloyd, G.L. Jackson, T.S. Taylor, E.A. Lazarus, T.C. Luce and R. Prater, "*Low voltage ohmic and electron cyclotron heating assisted startup in DIII-D"*, Nucl. Fusion **31** (1991) 2031

[15] Jayhyun Kim, S.W. Yoon, Y.M. Jeon, J.A. Leuer, N.W. Eidietis, D. Mueller, S. Park, Y.U. Nam, J. Chung, K.D. Lee, S.H. Hahn, Y.S. Bae, W.C. Kim, Y.K. Oh, H.L. Yang, K.R. Park, H.K. Na and the KSTAR Team, "*Stable plasma startup in the KSTAR device under various discharge conditions"*, Nucl. Fusion **51** (2012) 083034

[16] J. Bucalossi, F. Saint-Laurent, P. Hertout, M. Lennholm, F. Bouquey, C. Darbos and E. Traisne, "*Electron Cyclotron Resonance Heating Assisted Plasma Startup in the Tore Supra tokamak"*, Proc. 22nd Int. Conf. on Fusion Energy, Geneva, Switzerland, 2008 (Vienna, IAEA) (2008) EX/P6 – 12

[17] P.C. de Vries, A.C.C. Sips, H.T. Kim, P.J. Lomas, F. Maviglia, R. Albanese, I. Coffey, E. Joffrin, M. Lehnen, A. Manzanares, M. O'Mulane, I. Nunes, G. van Rooij, F.G. Rimini, M.F. Stamp and JET-EFDA Contributors, "*Characterisation of plasma breakdown at JET with a carbon and ITER-like wall"*, Nucl. Fusion **53** (2013) 053003

[18] J. Stober, G.L. Jackson, E. Ascasibar, Y.-S. Bae, J. Bucalossi, A. Cappa, T. Casper, M.-H. Cho, Y. Gribov, G. Granucci et al, "*ECH-assisted plasma startup with toroidally inclined launch: multi-machine comparison and perspectives for ITER"*, Nucl. Fusion **51** (2011) 083031

[19] Y.S. Bae, J.H. Jeong, S.I. Park, M. Joung, J.H. Kim, S.H. Hahn, S.W. Yoon, H.L. Yang, W.C. Kim, Y.K. Oh, A.C. England, W. Namkung, M.H. Cho, G.L. Jackson, J.S. Bak and the KSTAR team, "*ECH pre-ionization and assisted startup in the fully superconducting KSTAR tokamak using second harmonic"*, Nucl. Fusion **49** (2009) 022001

[20] B. Lloyd, P.G. Carolan and C.D. Warrick, "*ECH-assisted startup in ITER"*, Plasma Phys. Control. Fusion **38** (1996) 1627

[21] Hyun-Tae Kim, W. Fundamenski, A.C.C. Sips and EFDA-JET Contributors, "*Enhancement of plasma burn-through simulation and validation in JET"*, Nucl. Fusion **52** (2012) 103016

[22] Hyun-Tae Kim, A.C.C. Sips, P.C. de Vries, and JET-EFDA Contributors, "*Plasma burn-through simulations for ITER using DYON code"*, Plasma Phys. Control. Fusion **55** (2013) 124032

[23] J. Roth, W. Eckstein and M. Guseva, "*Erosion of Be as plasma-facing material"*, Fusion Eng. Des. **37** (1997) 465 – 80

[24] G.L. Jackson, T.A. Casper, T.C. Luce, D.A. Humphreys, J.R. Ferron, A.W. Hyatt, E.A. Lazarus, R.A. Moyer, T.W. Petrie, D.L. Rudakov and W.P. West, "*ITER startup studies in the DIII-D tokamak"*, Nucl Fusion **48** (2008) 125002

[25] G.L. Jackson, T.A. Casper, T.C. Luce, D.A. Humphreys, J.R. Ferron, A.W. Hyatt, J.A. Leuer, T.W. Petrie, F. Turco and W.P. West, "*Simulating ITER plasma startup and rampdown scenarios in the DIII-D tokamak"*, Nucl Fusion **49** (2009) 115027

[26] C.E. Kessel, S.M. Wolfe, I.H. Hutchinson, J.W. Hughes, Y. Lin, Y. Ma, D.R. Mikkelsen, F.M. Poli, M.L. Reinke, S.J. Wukitch and the C-Mod Team, "*Alcator C-Mod experiments in support of the ITER baseline 15 MA scenario"*, Nucl Fusion **53** (2013) 093021

[27] G. L. Jackson, P. A. Politzer, D. A. Humphreys, T. A. Casper, A. W. Hyatt, J. A. Leuer, J. Lohr, T. C. Luce, M. A. Van Zeeland, and J. H. Yu, *"Understanding and predicting the dynamics of tokamak discharges during startup and rampdown",* Phys. Plasmas **17** (2010) 056116; doi: 10.1063/1.3374242

[28] P.A. Politzer, G.L. Jackson, D.A. Humphreys, T.C. Luce, A.W. Hyatt and J.A. Leuer, "*Experimental simulation of ITER rampdown in DIII-D"*, Nucl Fusion **50** (2010) 035011

[29] A.C.C Sips, I. Voitsekhovitch, P. Lomas, I. Nunes, G. Saibene, and JET-EFDA Contributors, "*ITER Ramp-up and Ramp-down Scenarios Studies in Helium and Deuterium Plasmas in JET"*, Proc. 23rd Int. Conf. on Fusion Energy, Daejeon, Rep. of Korea, 2010 (Vienna, IAEA) (2010) EXC/P2-08

[30] C. Gormezano, A.C.C. Sips, T.C. Luce, S. Ide, A. Becoulet, X. Litaudon, A. Isayama, J. Hobirk, M.R. Wade, T. Oikawa, R. Prater, A. Zvonkov, et al, "*Chapter 6: Steady state operation"*, Nucl. Fusion **47** (2007) S285

[31] T.C. Luce, C.C. Petty and J.G. Cordey, "*Application of dimensionless parameter scaling techniques to the design and interpretation of magnetic fusion experiments"*, Plasma Phys. Control. Fusion **50** (2008) 043001

[32] P.N. Yushmanov, T. Takizuka, K.S. Riedel, O.J.W.F. Kardaun, J.G. Cordey, S.M. Kaye and D.E. Post, "*Scalings for tokamak energy confinement"*, Nucl. Fusion **30** (1990) 1999

[33] ITER Physics Expert Group on Confinement and Transport et al, "*Chapter 2: Plasma confinement and transport"*, Nucl. Fusion **39** (1999) 2175

[34] G.L. Jackson, F. Turco, T.C. Luce, R.J. Buttery, A.W. Hyatt, E.J. Doyle, J.R. Ferron, R.J. La Haye, P.A. Politzer, W.M. Solomon, and M.R. Wade, "*Long-pulse Stability Limits of ITER Baseline Scenario Plasmas in DIII-D"*, Proc. 24th Int. Conf. on Fusion Energy, San Diego, USA, 2012 (Vienna, IAEA) (2012) EX/P2-08

[35] A.C.C. Sips, G. Jackson, J. Schweinzer, S. Wolfe, J. Hobirk, H. Hoehnle, A. Hubbard, E. Joffrin, C. Kessel, P. Lomas, T. Luce, I. Nunes, J. Stober, JET EFDA Contributors, "*Demonstrating the ITER Baseline Operation at q_{95} = 3"*, Proc. 24th Int. Conf. on Fusion Energy, San Diego, USA, 2012 (Vienna, IAEA) (2012) ITR/P1-11

[36] J. Schweinzer, V. Bobkov, A. Burckhart, R. Dux, C. Fuchs, A. Kallenbach, J. Hobirk, C. Hopf, P.T. Lang, A. Mlynek, Th. Pütterich, F. Ryter, G. Tardini, J. Stober and the ASDEX Upgrade team, "*Demonstration of the ITER Baseline Scenario on ASDEX Upgrade"*, 40th EPS Conference on Plasma Physics, Espoo, Finland (2013) P2.134

[37] F. Turco and T.C. Luce, "*Impact of the current profile evolution on tearing stability of ITER demonstration discharges in DIII-D"*, Nucl. Fusion **50** (2010) 095010

[38] M.N.A. Beurskens, J. Schweinzer, C. Angioni, A. Burckhart, C.D. Challis, I. Chapman, R. Fischer, J. Flanagan, L. Frassinetti, C. Giroud, J. Hobirk et al, "*The Effect of a Metal Wall on Confinement in JET and ASDEX-Upgrade"*, Plasma Phys. Control. Fusion **55** (2013) 124043

[39] M.N.A. Beurskens, L. Frassinetti, C. Maggi, G. Calabro, B. Alper, C. Angioni, C. Bourdelle, S. Brezinsek, P. Buratti, C. Challis et al, ”*L-H Power Threshold, Confinement, and Pedestal Stability in JET with a Metallic Wall”*, Proc. 24th Int. Conf. on Fusion Energy, San Diego, USA, 2012 (Vienna, IAEA) (2012) EX/P7-20

[40] E. Joffrin, J. Bucalossi, P. Lomas, F. Rimini, R. Neu, I. Nunes, M. Baruzzo, M. Beurskens, C. Bourdelle, S. Brezinsek, et al, ”*Scenarios Development at JET with the New ITER-like Wall”*, Proc. 24th Int. Conf. on Fusion Energy, San Diego, USA, 2012 (Vienna, IAEA) (2012) EX/1-1

[41] W.M. Tang, ”*Microinstability-based model for anomalous thermal confinement in tokamaks”*, Nucl. Fusion **26** (1986) 1605

[42] T. Casper, Y. Gribov, ITER Domestic Agencies, and ITER collaborators, ”*Development of the ITER Baseline Inductive Scenario”*, Proc. 23rd Int. Conf. on Fusion Energy, Daejeon, Rep. of Korea, 2010 (Vienna, IAEA) (2010) ITR/P1-19

[43] A.R. Polevoi, N. Hayashi, H.S. Kim, S.H. Kim, F. Koechl, A.S. Kukushkin, V.M. Leonov, A. Loarte, S.Yu. Medvedev, M. Murakami, et al, ”*Optimisation of ITER Operational Space for Long-pulse Scenarios”*, 40th EPS Conference on Plasma Physics, Espoo, Finland (2013) P2.135

[44] D.P. Coster, X. Bonnin, B. Braams, H. Buerbaumer, E. Kaveeva, J.-W.Kim, A. Kukushkin, Y. Nishimura, D. Reiter, V. Rozhansky, R. Schneider, B. Scott, S. Voskoboynikov and the ASDEX Upgrade team, ”*Further developments of the edge transport simulation package, SOLPS”*, Proc. 19th Int. Conf. on Fusion Energy, Lyon, France, 2002 (Vienna, IAEA) (2002) TH/P2-13

[45] A.S. Kukushkin, H.D. Pacher, V. Kotov, D. Reiter, D. Coster and G.W. Pacher, "*Effect of neutral transport on ITER divertor performance"*, Nucl. Fusion **45** (2005) 608

[46] P.B. Snyder, R.J. Groebner, J.W. Hughes, T.H. Osborne, M. Beurskens, A.W. Leonard, H.R. Wilson and X.Q. Xu, "*A first-principles predictive model of the pedestal height and width: development, testing and ITER optimization with the EPED model"*, Nucl. Fusion **51** (2011) 103016

[47] J.A. Crotinger, L. LoDestro, L.D. Pearlstein, A. Tarditi, T.A. Casper, E. Bickford Hooper, "*CORSICA: A Comprehensive Simulation of Toroidal Magnetic-Fusion Devices"*, Lawrence Livermore National Laboratory Report UCRL-ID-126284 (1997) NTIS #PB2005-10215

[48] S. Wiesen, *"JINTRAC-JET modelling suite",* JET ITC-Report 2008 (2008), http://www.eirene.de/JINTRAC_Report_2008.pdf

[49] Y.R. Martin, T. Takizuka and ITPA CDBM H-mode Threshold Database Working Group, "*Power requirement for accessing the H-mode in ITER"*, Journal of Physics: Conference Series **123** (2008) 12033

[50] E. Righi, D.V. Bartlett, J.P. Christiansen, G.D. Conway, J.G. Cordey, L.-G. Eriksson, H.P.L. De Esch, G.M. Fishpool, C.W. Gowers, J.C.M. de Haas et al, "*Isotope scaling of the H mode power threshold on JET"*, Nucl. Fusion **39** (1999) 309

[51] G. Pereverzev and P.N. Yushmanov, "*ASTRA Automated System for Transport Analysis"*, IPP Report 5/98 (2002)

[52] Yong-Su Na, C.E. Kessel, J.M. Park, Sumin Yi, A. Becoulet, A.C.C. Sips and J.Y. Kim, "*Simulations of KSTAR high performance steady state operation scenarios"*, Nucl. Fusion **49** (2009) 115018

[53] J.F. Artaud, V. Basiuk, F. Imbeaux, M. Schneider, J. Garcia, G. Giruzzi, P. Huynh, T. Aniel, F. Albajar, J.M. Ané et al, "*The CRONOS suite of codes for integrated tokamak modelling"*, Nucl. Fusion **50** (2010) 043001

[54] H. St. John, T.S. Taylor, Y.R. Lin-Liu, A.D. Turnbull, "*Transport Simulations of Negative Magnetic Shear Discharges"*, Proc. 15th Int. Conf. on Fusion Energy, Seville, Spain, 1994 (Vienna, IAEA) (1994) **Vol. 3** p. 603

[55] J.M. Park, E.J. Doyle, J.R. Ferron, C.T. Holcomb, G.L. Jackson, L.L. Lao, T.C. Luce, L.W. Owen, M. Murakami, T.H. Osborne, P.A. Politzer, R. Prater, and P.B. Snyder, " *Experiment and Modeling of ITER Demonstration Discharges in the DIII-D Tokamak"*, Proc. 23rd Int. Conf. on Fusion Energy, Daejeon, Rep. of Korea, 2010 (Vienna, IAEA) (2010) EXC/P2-05

[56] H. Shirai, T. Takizuka, Y. Koide, O. Naito, M. Sato, Y. Kamada and T. Fukuda, "*Non-dimensional transport study on ELMy H-mode plasmas in JT-60U"*, Plasma Phys. Control. Fusion **42** (2000) 1193

[57] N. Hayashi, T. Takizuka and T. Ozeki, "*Profile formation and sustainment of autonomous tokamak plasma with current hole configuration"*, Nucl. Fusion **45** (2005) 933

[58] C.E. Kessel, R.E. Bell, M.G. Bell, D.A. Gates, S.M. Kaye, B.P. LeBlanc, J.E. Menard, C.K. Phillips, E.J. Synakowski, G. Taylor, R. Wilson, R.W. Harvey, T.K. Mau, P.M.

Ryan, and S.A. Sabbagh, ”*Long pulse high performance plasma scenario development for the National Spherical Torus Experiment”*, Phys. Plasmas **13** (2006) 056108

[59] J.E. Kinsey, G.M. Staebler, and R.E. Waltz, ”*Predicting core and edge transport barriers in tokamaks using the GLF23 drift-wave transport model”*, Phys. Plasmas **12** (2005) 052503

[60] G. Giruzzi, J.M. Park, M. Murakami, C.E. Kessel, A. Polevoi, A.C.C. Sips, J.F. Artaud, V. Basiuk, P. Bonoli, R.V. Budny et al, ”*Integrated modeling of steady-state scenarios for ITER: physics and computational challenges”*, Proc. 22nd Int. Conf. on Fusion Energy, Geneva, Switzerland, 2008 (Vienna, IAEA) (2008), IT/P6-4

[61] T. Oikawa, J.M. Park, A.R. Polevoi, M. Schneider, G. Giruzzi, M. Murakami, K. Tani, A.C.C. Sips, C. Kessel, W. Houlberg et al, ”*Benchmarking of Neutral Beam Current Drive Codes as a Basis for the Integrated Modeling for ITER”*, Proc. 22nd Int. Conf. on Fusion Energy, Geneva, Switzerland, 2008 (Vienna, IAEA) (2008) IT/P6-5

[62] M. Schneider, L.-G. Eriksson, I. Jenkins, J.F. Artaud, V. Basiuk, F. Imbeaux, T. Oikawa, JET-EFDA contributors and ITM-TF contributors, ”*Simulation of the neutral beam deposition within integrated tokamak modelling frameworks”*, Nucl. Fusion **51** (2011) 063019

[63] J. García, G. Giruzzi, J.F. Artaud, V. Basiuk, J. Decker, F. Imbeaux, Y. Peysson, and M. Schneider, ”*Critical Threshold Behavior for Steady-State Internal Transport Barriers in Burning Plasmas”*, Phys. Rev. Lett. **100** (2008) 255004

[64] T.C. Luce, ”*Reflections on ITER Steady-State Scenario Operational Space”*, Presented at the 1st Integrated Operational Scenarios Topical Group Meeting of the ITPA, 20 October 2008 (2008)

[65] Y. Shimomura, Y. Murakami, A.R. Polevoi, P. Barabaschi, V. Mukhovatov and M. Shimada, *"ITER*: *Opportunity of burning plasma studies",* Plasma Phys. Control. Fusion **43** (2001) A385

[66] B.J. Green for the ITER International Team and Participant Teams, "*ITER: burning plasma physics experiment"*, Plasma Phys. Control. Fusion **45** (2003) 687 – 706

[67] E.J. Doyle, J.C. DeBoo, J.R. Ferron, G.L. Jackson, T.C. Luce, M. Murakami, T.H. Osborne, J.-M. Park, P.A. Politzer, H. Reimerdes, R.V. Budny, T.A. Casper, C.D. Challis, R.J. Groebner, C.T. Holcomb, A.W. Hyatt, R.J. La Haye, G.R. McKee, T.W. Petrie, C.C. Petty, T.L. Rhodes, M.W. Shafer, P.B. Snyder, E.J. Strait, M.R. Wade, G. Wang, W.P. West and L. Zeng, "*Demonstration of ITER operational scenarios on DIII-D"*, Nucl. Fusion **50** (2010) 075005

[68] S.C. Jardin, J.L. DeLucia, N. Pomphrey, "*Dynamic modeling of transport and positional control of tokamaks."*, J. Comput. Phys. **66** (1986) 481

[69] R.J. Hawryluk, "*An empirical approach to tokamak transport"*, Physics of Plasmas Close to Thermonuclear Conditions, ed B. Coppi et al (Brussels: Commission of the European Communities) **vol 1** (1980) pp 19 – 46

[70] D. Bora for the ITER Organisation, "*RF heating needs and plans for ITER"*, 17th Topical Conference on Radio Frequency Power in Plasmas, Clearwater, Florida, AIP Conference Proceedings 933 (2007) pp. 25-32

[71] C.C. Petty, "*Sizing up plasmas using dimensionless parameters"*, Phys. Plasmas **15** (2008) 080501

[72] J.E. Rice, A. Ince-Cushman, J.S. deGrassie, L.-G. Eriksson, Y. Sakamoto, A. Scarabosio, A. Bortolon, K.H. Burrell, B.P. Duval, C. Fenzi-Bonizec, M.J. Greenwald, R.J. Groebner, G.T. Hoang, Y. Koide, E.S. Marmar, A. Pochelon and Y. Podpaly, *"Inter-machine comparison of intrinsic toroidal rotation in tokamaks"*, Nucl. Fusion **47** (2007) 1618

[73] W.M. Solomon, K.H. Burrell, J.S. deGrassie, J.A. Boedo, A.M. Garofalo, R.A. Moyer, S.H. Muller, C.C. Petty and H. Reimerdes, *"Characterization of intrinsic rotation drive on DIII-D"*, Nucl. Fusion **51** (2011) 073010